JOURNAL OF GEOPHYSICAL RESEARCH, VOL. 105, NO. B1, PAGES 463–481, JANUARY 10, 2000

Basal mechanics of Ice Stream B, West Antarctica
1. Till mechanics

Slawek Tulaczyk,[1] W. Barclay Kamb, and Hermann F. Engelhardt

Division of Geological and Planetary Sciences, California Institute of Technology, Pasadena, California

Abstract. Data from laboratory geotechnical tests on till recovered from beneath Ice Stream B, West Antarctica, at the Upstream B camp (hereinafter the UpB till) show that failure strength of this till is strongly dependent on effective stress but is practically independent of strain and strain rate. These data support use of a Coulomb-plastic rheology in modeling of ice stream behavior and subglacial till deformation. Our testing program combined triaxial, ring shear, and confined uniaxial tests to investigate till strength and compressibility. Results show that the UpB till follows closely Coulomb's equation in which shear strength is a linear function of normal effective stress (apparent cohesion near zero and internal friction angle ϕ equal to 24°). Till compressibility is best described by a logarithmic function that relates void ratio to normal effective stress. In general, the behavior of the UpB till is consistent with other experimental evidence regarding mechanical behavior of granular materials. Based on our laboratory results we formulate the Compressible-Coulomb-Plastic till model in which there are three interrelated, primary state variables: shear strength, void ratio, and normal effective stress. This model is used in the second part of our study to simulate response of subglacial till to realistic effective stress forcings. These simulations demonstrate that the model is capable of reproducing fundamental aspects of subglacial till kinematics: (1) occurrence of tilt rate oscillations and negative tilt rates in tiltmeter records, and (2) distributed till deformation to depths of 0.1 - 1.0 m beneath the ice base. Our laboratory and modeling results substantiate application of the Compressible-Coulomb-Plastic model in simulations of the motion of Ice Stream B over its weak till bed.

1. Introduction

Glaciological and geophysical studies indicate that fast motion of West Antarctic ice streams is possible because of an efficient basal lubrication provided by a layer of weak subglacial till (Figures 1 and 2) [*Alley et al.*, 1986, 1987a, b; *Blankenship et al.*, 1986, 1987; *Engelhardt et al.*, 1990; *Kamb*, 1991]. Due to this lubrication, these ice streams move roughly 100 times faster than the rest of the ice sheet, ~100 m yr^{-1} versus ~1 m yr^{-1}, and carry the majority of ice discharging from West Antarctica [*Bentley*, 1987; *Whillans and van der Veen*, 1993]. One of the most perplexing characteristics of the West Antarctic ice streams is that their fast motion is accomplished under relatively low driving stresses, ~1-30 kPa versus 50-150 kPa for typical glaciers and ice sheets [*Bentley*, 1987; *Paterson*, 1994]. Construction of a well-constrained and self-consistent physical model of fast ice stream motion represents one of the most pressing tasks of modern glaciology [*Alley et al.*, 1987a, b; *Clarke*, 1987a]. Without a model of this kind it is difficult to make reliable predictions regarding the future of the possibly unstable West Antarctic Ice Sheet [*Bentley*, 1997; *Bindschadler*, 1997, 1998; *MacAyeal*, 1992]. Improved understanding of ice stream mechanics is also needed to reconstruct the behavior of Pleistocene ice masses and to understand their role in triggering regional and global climatic changes [*Clark*, 1992; *Hughes*, 1996].

In the past, models of ice stream motion over deformable tills have been based on the assumption that till behaves as a viscous or Bingham fluid with a linear or mildly nonlinear strain rate dependence of strength [e.g., *Alley et al.*, 1986, 1987a, b; *MacAyeal*, 1992]. These initial decisions to use the viscous or Bingham till model were based on the conjecture that the sub-ice stream till is similar in its mechanical behavior to the till from beneath Breidamerkurjokull glacier, Iceland, whose in situ deformation was investigated by *Boulton and Hindmarsh* [1987]. Since its publication, their report was used to justify an assumption of viscous till behavior in numerous glaciological and glacial geological studies [e.g., *Clark*, 1992; *Cuffey and Alley*, 1996] (see review by *Murray* [1998]). Only after samples of the weak till have been recovered from beneath Ice Stream B at the camp Upstream B (hereinafter the UpB till), direct investigations of the rheology of sub–ice stream tills became possible (Figure 1b) [*Engelhardt et al.*, 1990]. *Kamb* [1991] used strain rate-controlled and stress-controlled shear box tests to determine the strain rate dependence of till strength. In contrast to predictions of the widely used viscous till model, the tested till samples behaved in a nearly plastic manner, that is, exhibited almost no strain rate dependence of strength. The difference between the viscous predictions and plastic laboratory observations was so strong that it has raised doubts that, for some reason, soil mechanics tests yield results that are not representative of in situ till behavior.

[1]Now at Department of Geological Sciences, University of Kentucky, Lexington.

Copyright 2000 by the American Geophysical Union.

Paper number 1999JB900329.
0148-0227/00/1999JB900329$09.00

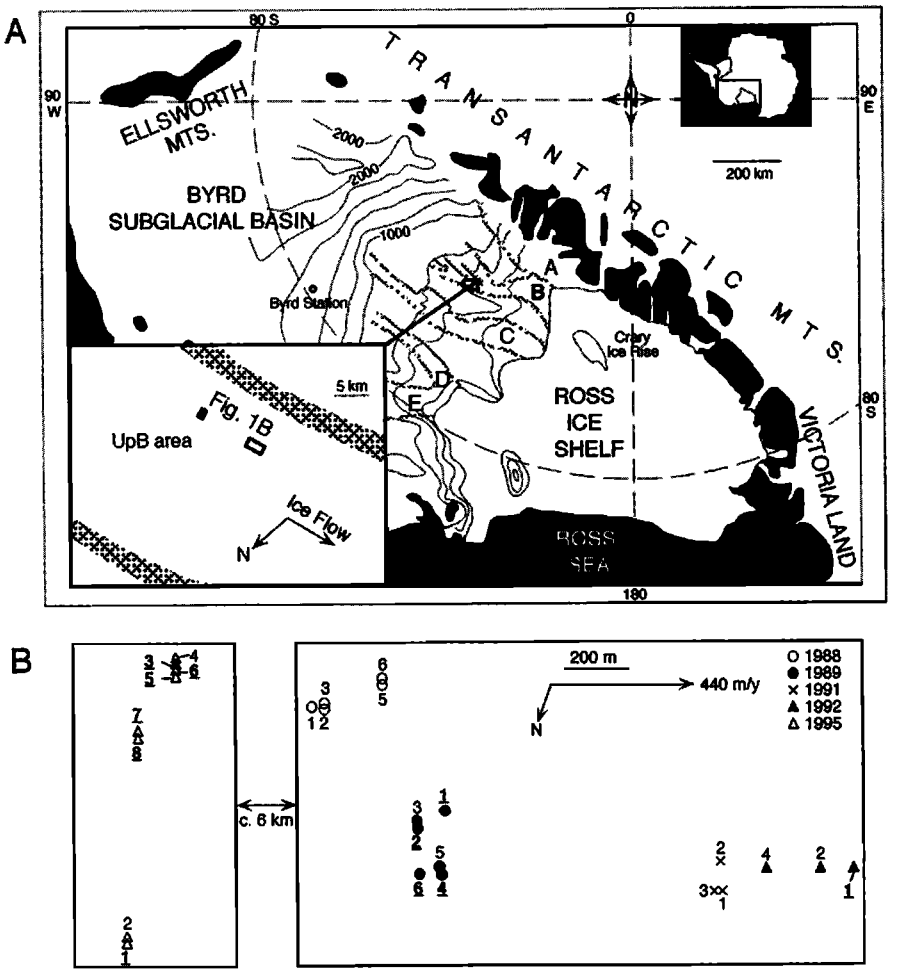

Figure 1. (a) Letters A through E denote the individual ice streams flowing through the Ross Sea section of West Antarctica. Location map shows outlines of the ice streams, ice elevation contour lines (250 m interval), and major mountain ranges [after *Tulaczyk et al.*, 1998, Figure 1]. (b) Locations of boreholes drilled on Ice Stream B in the UpB area during field seasons 1988-1995, shown in a stationary, geographic reference frame (the reference frame of the ice surface is moving 440 m yr^{-1} at UpB [*Whillans and van der Veen*, 1993]). Individual boreholes are labeled with consecutive numbers indicating order of drilling during a given field season. The label numbers for these boreholes from which sediment cores were acquired are bold and underlined.

Since the publication of *Kamb* [1991] our research group has had the opportunity to hear various concerns regarding the validity of the soil mechanics approach to studying and modeling deformation of subglacial tills. One line of criticism explored two potential limitations of shear box tests used by *Kamb* [1991]: (1) the relatively small strain that may be unable to reproduce real subglacial conditions and (2) the supposition that nearly plastic till rheology observed in shear box tests is not an inherent property of the till itself but an artifact of the geometry of the apparatus which forces development of a thin "plastic" shear zone (~1 mm in thickness). However, the most potent argument against plastic rheology of subglacial tills was provided by the claim that deformation in a plastic till could not distribute throughout any significant thickness but would collapse to a single shear plane [e.g., *Alley*, 1993]. Strain markers and tiltmeters emplaced in till layers beneath a number of mountain glaciers have conclusively shown that deformation does distribute in these tills, at least to depths of several decimeters [*Blake*, 1992; *Blake et al.*, 1994; *Boulton and Hindmarsh*, 1987; *Hooke et al.*, 1997; *Iverson et al.*, 1995]. Nonetheless, recent studies of such distributed till deformation beneath two mountain glaciers have failed to confirm that this strain distribution can be attributed to nearly linearly viscous till rheology [*Blake*, 1992, pp. 62-63; *Hooke et al.*, 1997; *Iverson et al.*, 1995]. Results of one borehole experiment from Ice Stream B indicate even that in the sub-ice stream environment, vertical strain distribution may be itself quite small with most of the ice stream motion being accommodated by sliding along the ice-till interface [*Engelhardt and Kamb*, 1998].

Amidst this array of seemingly contradictory observations and models remains the pressing need to resolve the dilemma of till mechanics whose proper understanding must precede construction of reliable models of coupled ice-till motion. From the point of view of ice dynamics the question whether till is a mildly nonlinear or nearly plastic material is nontrivial because instability of ice-till systems increases with the degree of till nonlinearity [*Kamb*, 1991]. Therefore we have continued our efforts to study the mechanics of the UpB till in the laboratory and to build experimentally based models of till mechanics that can explain important aspects of in situ till deformation, including the vertical distribution of strain in till. In this manuscript we report the re-

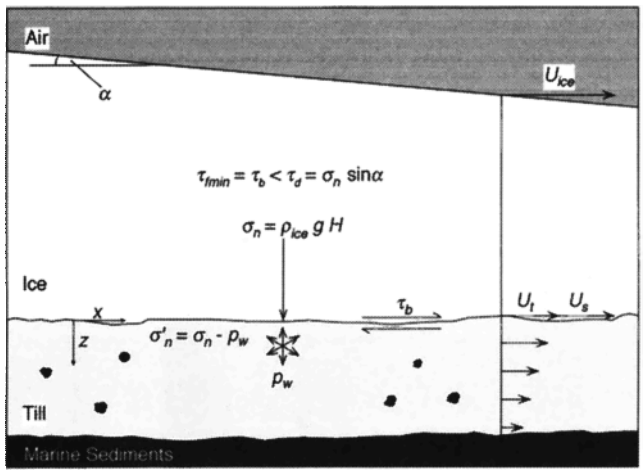

Figure 2. Schematic vertical cross section through Ice Stream B, not to scale. In the lower left we show the two-dimensional, *x-z* coordinate system used in this manuscript. The large vertical arrow indicates the ice load σ_n acting on the top of the till. This ice load less the basal water pressure is the normal effective stress σ'_n at the ice-till interface. The ice stream flow is driven by the gravitational driving stress τ_d which represents the downslope component of the gravitational force on the ice (per unit area) integrated over the ice thickness. A part of the driving stress is supported by the basal shear stress τ_b that is assumed here to be equal to the minimum till strength τ_{fmin}. The ice-stream flow velocity U_{ice} is composed of a till-deformation component U_t and a basal sliding component U_s that occurs as a relative motion along the ice-till interface.

sults of new laboratory and modeling investigations. Based on these results, we reject the hypothesis that there is a real disparity between till behavior in situ and in laboratory tests. We propose a new model for the mechanics of the UpB till that is based on results of geotechnical tests, and in a companion manuscript we show that this model of till mechanics may be successfully used in ice stream modeling [*Tulaczyk et al.*, this issue].

2. Relevant Concepts From Soil Mechanics

Soils represent a mixture of fluids and rigid particles, and deformation of this mixture is inevitably a complex process. Because of this complexity it is not possible to develop a completely generalized model of soil behavior. Rather, specifics of any soil mechanics model must be chosen to fit the particular problem of interest and the required accuracy of solutions [*Whittle and Kavvadas*, 1994]. Our work was driven by the desire to construct a mechanical model of the UpB till that can be used to (1) explain the first-order aspects of observed subglacial till kinematics (this paper), and (2) incorporate realistic treatment of ice-till interactions into an ice stream model [*Tulaczyk et al.*, this issue]. Our objective is to arrive at simple models that are justified by the results of laboratory tests and are able to reproduce fundamental features of field observations without turning to use of unconstrained, adjustable parameters.

As part of our drive towards simplifying the considered problems, we forego the use of the stress tensor in favor of a relatively simple two-dimensional stress state which consists of the shear stress τ and the normal effective stress σ'_n. This simple stress state relates directly to the subglacial stress state that acts upon a till layer in nature (Figure 2) and is convenient because it permits separate investigations of till response to the normal effective stress and the shear stress.

Figure 3 shows a few basic aspects of soil behavior that will become important in our treatment of till mechanics. First, we illustrate the concept of a failure strength τ_f that is typically reached only after an initial, transient period of strain hardening or strength mobilization (Figure 3a). In heavily overconsolidated and in clay-rich soils, the initial strain hardening is followed by a less pronounced strain weakening giving rise to a transient peak strength (dashed line in Figure 3a). The steady state reached after all of the transient stress-strain trends have ceased is referred to as the critical, residual, or ultimate state [*Bishop et al.*, 1971; *Schofield and Wroth*, 1968, p. 19]. As illustrated in Figure 3b, soils are frictional materials and their failure strength along a given shear plane is determined by the effective stress acting normal to the shear plane [*Terzaghi et al.*, 1996, equation 17.4]:

$$\tau_f = c_a + \sigma'_n \tan\phi = c_a + (\sigma_n - p_w) \tan\phi, \quad (1)$$

where c_a is the apparent cohesion, ϕ is the internal friction angle, σ_n is the total normal stress, $\sigma'_n = \sigma_n - p_w$ is the effective normal stress, and p_w is the pore pressure.

The complexity of soil behavior is rooted to a great extent in the ability of soils to change water content under different effective stresses [*Wood*, 1992, pp. 4-5]. Soil compressibility depends on the effective stress history of a given soil sample. In this regard a soil may be in one of two states: (1) normally consolidated or "virgin" state in which the current effective stress is higher than any effective stresses to which the soil was subjected in the past, $\sigma'_n = \sigma'_{nmax}$ and (2) an overconsolidated state in which $\sigma'_n < \sigma'_{nmax}$ (Figure 3c). It is important to note here that the latter usage of the term "overconsolidation" is more general than its usage in geosciences where overconsolidation typically implies removal of some of the preexisting overburden. For example, fluctuations of water pressure in a subglacial environment are sufficient to induce overconsolidation in till; no decrease in ice thickness is necessary.

When plotted on graphs of void ratio versus logarithm of the effective normal stress, typical volume change data for soils can be approximated by straight lines (Figure 3c) [*Scott*, 1963, p. 174]:

$$e = e_o - C_\xi \log(\sigma'_n / \sigma'_{no}), \quad (2)$$

where $e = V_w/V_s$ is the void ratio obtained by dividing the pore volume by the volume of solids (void ratio is related to porosity through $n_p = e/(1 + e)$), e_o is the void ratio at the reference value of effective normal stress, σ'_{no} = 1 kPa, and C_ξ is the dimensionless coefficient of compressibility. The subscript ξ is replaced by c (for "consolidation") and by s (for "swelling") to indicate the coefficient of compressibilities in the virgin and overconsolidated states, respectively. The line that describes soil behavior in the virgin state is commonly designated as the normal consolidation line (NCL) and it corresponds to the loosest possible state for a soil at a given normal effective stress [*Clarke*, 1987b; *Schofield and Wroth*, 1968, p. 72]. The lines that approximate volume change behavior of overconsolidated soils are referred to as the unloading-reloading lines (URL). Consolidation is large and mostly irrecoverable in the virgin state because it involves predominantly permanent rearrangement of particles. Under the condition of overconsolidation the converse is true; deformations are mainly elastic in nature with a small component of permanent changes. Because of the predominance of elastic effects in the overconsolidated state, consolidation and swelling

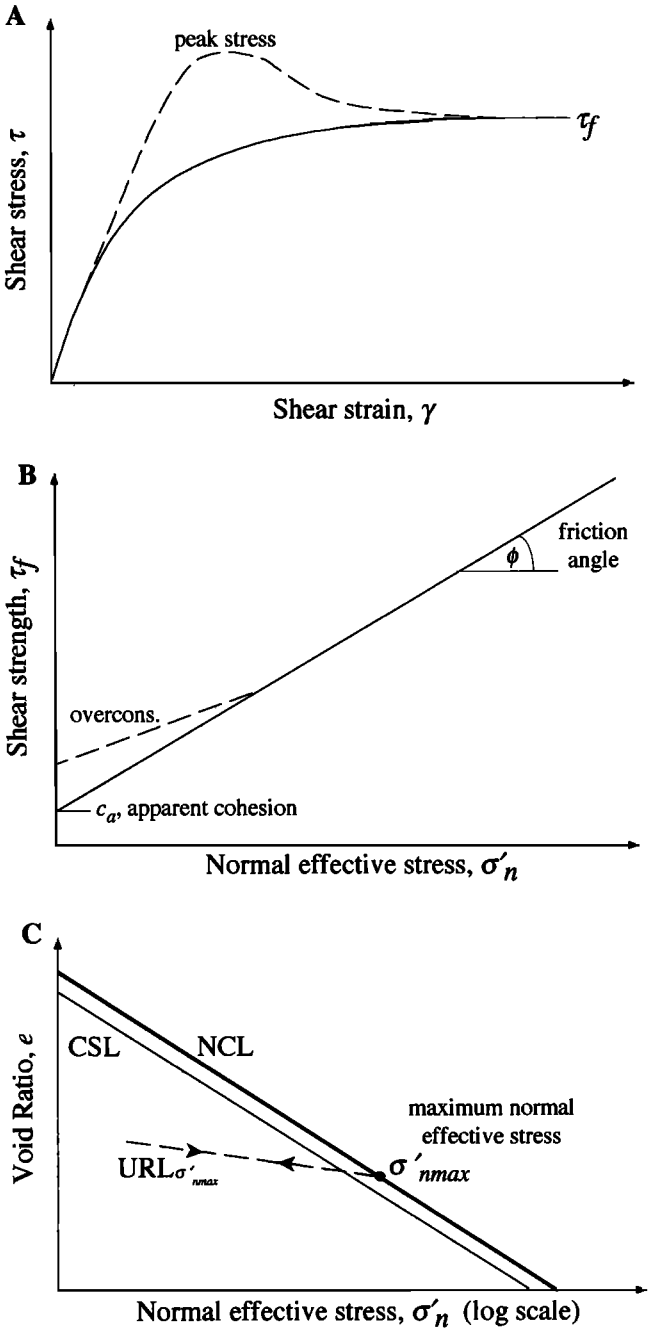

Figure 3. Simplified representation of typical soil behavior in terms of the relationships between (a) shear stresses and shear strains, (b) shear strength and normal effective stress, and (c) void ratio and normal effective stress (compiled and modified from *Clarke* [1987b], *Schofield and Wroth* [1968, pp. 19 and 72-73], *Scott* [1963 p. 174], *Tulaczyk* [1999], and *Wood* [1992 p. 141]). All symbols and concepts are explained in the text.

may be approximated to the first order by the same line (e.g., URL in Figure 3c) [*Schofield and Wroth*, 1968, pp. 72-73; *Wood*, 1992, section 3.3].

The virgin and overconsolidated states represent "static" conditions of negligible shear strain. Prolonged shearing of soils leads to the so-called "critical state" in which a condition of a volumetric steady state is reached after transient volume changes at small strains [*Schofield and Wroth*, 1968, p. 19]. In the e -log σ'_n space, the critical state of a shearing soil is represented by the critical state line (CSL in Figure 3c) [*Clarke*, 1987b; *Wood*, 1992, p. 141]. In general, the CSL lies parallel to and slightly below the NCL [*Clarke*, 1987b, Figure 1; *Jones*, 1992, Figure 2.25; *Karig and Morgan*, 1992, Figure 6-13]. The CSL cuts the half-space below the NCL into two distinct regions. If a soil sample is initially in the upper region, that is, it is normally consolidated or lightly overconsolidated, this sample will consolidate during shear. However, if a soil sample is below the CSL, that is, it is heavily overconsolidated, this sample will dilate if sheared.

After providing the basic background on soil compressibility and overconsolidation, we can now show how to calculate the peak strength of overconsolidated soils (dashed lines in Figures 3a and 3b). We do this using the Hvorslev failure criterion [*Wood*, 1992, equation 7.40]:

$$\tau_{fov} = c_{ne}\,\sigma'_{ne} + \sigma'_n \tan\phi_e, \qquad (3)$$

where τ_{fov} is the peak strength of overconsolidated soil, σ'_{ne} is the equivalent consolidation stress, c_{ne} is the effective cohesion, and ϕ_e is the effective internal friction angle. The two latter terms are frequently referred to as the Hvorslev strength parameters that are analogous to the Coulomb parameters in (1), except that c_{ne} is here a dimensionless quantity. The equivalent consolidation stress is obtained by horizontally projecting the void ratio of an overconsolidated soil sample e_{ov} onto the NCL and reading off the corresponding effective stress:

$$\sigma'_{ne} = \sigma'_{no}\, 10^{(e_o - e_{ov})/C_c}, \qquad (4)$$

where e_o and C_c are the parameters of the NCL (equation (2)). Experiments indicate that light overconsolidation does not produce a significant increase in soil strength [*Wood*, 1992, Figures 7.21 and 7.22]. Therefore the Hvorslev failure criterion should be used instead of the Coulomb failure criterion only when the soil overconsolidation ratio is greater than 2 [*Wood*, 1992, pp. 198-203]. The overconsolidation ratio is defined as the ratio of past maximum effective stress to the current normal effective stress, $OVR = \sigma'_{nmax}/\sigma'_n$.

3. Till Sampling and Laboratory Procedures

As part of a drilling project focused on investigations of ice stream mechanics [*Engelhardt and Kamb*, 1998; *Engelhardt et al.*, 1990; *Jackson and Kamb*, 1997; *Kamb*, 1991], 12 till cores and a number of smaller till samples were acquired from beneath Ice Stream B (ISB) in the UpB area between 1988 and 1995 (Figure 1b). The spacing of till sampling sites varied from as little as several meters up to ~8 km. The till cores were recovered using a 6-m-long piston corer. Their lengths range between ~0.3 and 3.0 m. Sedimentological analyses of these cores showed that the sampled subglacial material is fairly homogeneous. On average, the core material was composed of 35% clay, 23% silt, 35% sand, and 7% of granules and pebbles (based on 35 samples) [*Tulaczyk et al.*, 1998]. The sedimentological properties of the core material are consistent with the conclusion that our cores have sampled the widespread till layer whose presence beneath ISB has been previously inferred from seismic data [*Blankenship et al.*, 1986, 1987].

To study the mechanical behavior of the till, we performed a sequence of laboratory tests guided by the standard procedures for soil testing [*Bishop and Henkel*, 1957; *Bowles*, 1992]. The main part of the mechanical testing program was based on triaxial, ring shear, and confined uniaxial tests, as follows.

Six out of a total of seven triaxial compression tests were done under undrained conditions (U1, U2, U3, R1, R2, and R3) and one under drained conditions (D1). Undrained tests were chosen as the main mode of triaxial testing because they can be performed over much shorter time periods (hours versus days) if a clay-rich, low-permeability material, such as the UpB till, is being analyzed [*Bowles*, 1992, p. 191]. At the same time, extensive experimental studies have shown that results of undrained tests do not differ significantly from the results of drained tests provided that interpretation of triaxial test results is done in terms of effective stresses [*Bishop and Henkel*, 1957, pp. 19-20; *Scott*, 1963, p. 374]. The single drained test was performed mainly to provide additional constraints on the volume-effective stress behavior of the UpB till.

We used undisturbed till samples in the first three tests (U1-3). The samples were "undisturbed" in the sense that they were extracted from the core liner just before testing without any intentional remolding. However, microscopic examination of till thin sections suggests that the samples had experienced disturbance during acquisition from the sub-ice stream environment via piston coring. The three "undisturbed" samples were taken in 10-cm-long, 5-cm-diameter sections from the depth range of ~1.5-2.5 m in core 92-1 (Figure 1b). Independent measurements show that in this part of the core, the pre test till porosity was 0.369 to 0.392 (void ratio 0.585 to 0.645). During the undrained and drained triaxial compression tests we have followed procedures described by *Bishop and Henkel* [1957] and *Bowles* [1992, pp. 165-200]. The following physical parameters were measured in the triaxial tests: (1) pore pressure (undrained tests only), (2) water gain/loss (drained test only), (3) axial load, (4) axial displacement, and (5) radial pressure. The second set of three triaxial tests (R1, R2, and R3) followed the same procedures but used till samples that were thoroughly remolded and reconstituted to porosity of ~0.4. These tests were designed primarily to determine the influence of strain rate on till strength. The axial displacement rate was varied over 4 orders of magnitude (axial velocity of 1.35×10^{-8} to 1.27×10^{-4} m s^{-1}). Finally, for comparison with the six undrained tests, we performed one triaxial test in which drainage was allowed during shear (D1). The axial deformation rate at which a sample of the UpB till should experience drained conditions can be estimated using standard procedures [*Bishop and Henkel, 1957*, p. 126-127]. Given the low hydraulic diffusion coefficient for this till, $c_v \cong 10^{-8}$ m^2 s^{-1} [*Tulaczyk*, 1998, chapter 5], the axial velocity must be less than 2.5×10^{-7} m s^{-1}, strain rate of ~3×10^{-6} s^{-1}). The volume of water that had entered or exited the sample was read manually every 5 minutes using a burette (estimated reading error of ± 0.01 cm^3 with total drainage of a few cubic centimeters).

In triaxial tests the total axial strain is limited typically to 0.1 to 0.2. To determine whether the strength of the UpB till changes significantly with strain, we constructed a small ring shear device in which the material was sheared to much greater strains. Our device is similar to the Bromhead apparatus used extensively for soil testing in the United Kingdom [*Anayi et al.*, 1989; *Bromhead*, 1979; *Stark and Vettel*, 1992]. The lower plate of the device contains a sample chamber 2.9 cm wide, 1 cm deep, and with 17.4 cm centerline diameter and is moved by an electrical motor with a speed control box. With this device we can test only remolded samples. Prior to testing, all particles with diameter greater than 2 mm were removed by wet sieving. This coarse fraction constituted 7 wt % of the till solids. After the till sample is loaded into the chamber, the upper plate is placed on top, held with a square shaft so that it cannot rotate horizontally but can move up and down, and loaded with dead weight to achieve a desired normal stress. Thinning of the till sample caused by application of the normal load is monitored with displacement transducers. Once the sample stops consolidating, the lower plate with the sample is rotated at a constant rate with respect to the fixed upper plate. Shearing takes place in the till sample and the shear stress is measured with precision of ±0.01 kPa (over 0-100 kPa range). Further details regarding testing of till in ring shear devices are given in *Iverson et al.* [1997] and *Tulaczyk* [1998, chapter 4].

Confined uniaxial tests were used to investigate consolidation/swelling of UpB till samples in response to increase/decrease in normal effective stress [*Bowles*, 1992, pp. 129-154]. Sample thinning and thickening was monitored via a dial indicator with a precision of 0.025 mm in a total displacement range of 25.4 mm. Our water content measurements on samples from this and other geotechnical tests followed standard procedures [*Bowles*, 1992, pp. 15-18]. Water content is recalculated into porosity and void ratio using the previously established density of till solids ρ_s = 2640 kg m^{-3} (H. Engelhardt, unpublished data, 1990), and assuming water density ρ_w = 1000 kg m^{-3}.

4. Laboratory Results

In this section, we discuss the results of geotechnical tests on samples of the UpB till and compare them to the existing mechanical models of till and soil behavior [e.g., *Boulton and Hindmarsh*, 1987; *Clarke*, 1987b; *Schofield and Wroth*, 1968; *Wood*, 1992].

4.1. Strain-Strength Relationship

As observed previously by *Kamb* [1991] in shear box tests, a sheared sample of the UpB till experiences a transient period of strength mobilization before it reaches a more or less steady strength (Figure 4a). Our triaxial tests show that effective stress and pore pressure experience similar transient changes at small strains (0.01 to 0.1 strains). Figure 4a shows relevant examples from the test U2. The other six triaxial tests yielded analogous results (raw data by *Tulaczyk* [1998, chapter 4]). These results are in agreement with published outcomes of triaxial tests performed on other tills which have reached failure stress at as little as 0.04 axial strain (~0.055 shear strain) [*Bishop and Henkel*, 1957, Tables 2 and 8].

The results of our large-strain ring shear tests (Figures 4b and 4c) demonstrate still more convincingly that there is little change in till strength with strain; even for strains that are orders of magnitude greater than the strains accumulated in triaxial or shear box tests. There is a small peak in strength early in our ring shear tests on the UpB till. Afterwards, till strength drops off to an "ultimate" or "residual" value (Figure 4b). This behavior is typical for clay-rich soils [*Bishop et al.*, 1971; *Skempton*, 1985; *Stark and Vettel*, 1992, Figure 6]. In our two ring shear tests, the difference between the peak and the "ultimate" coefficient of internal friction for the UpB till was only 6% (Figure 4b) and 8% (triangles in Figure 4c). The small magnitude of these drop-offs is comparable to that observed in ring shear tests on other soils with index properties similar to that of the till (index of plasticity I_p = 15 to 16%, liquid limit, LL = 34 to 35%, and plastic limit, PL = 18%; see *Mitchell* [1993, Figure 14.51]). Recently, *Iverson et al.* [1997] tested a till sample containing 32% of clay size particles (versus 35% in the UpB till) and also observed a post-peak drop-off in strength of only 7%.

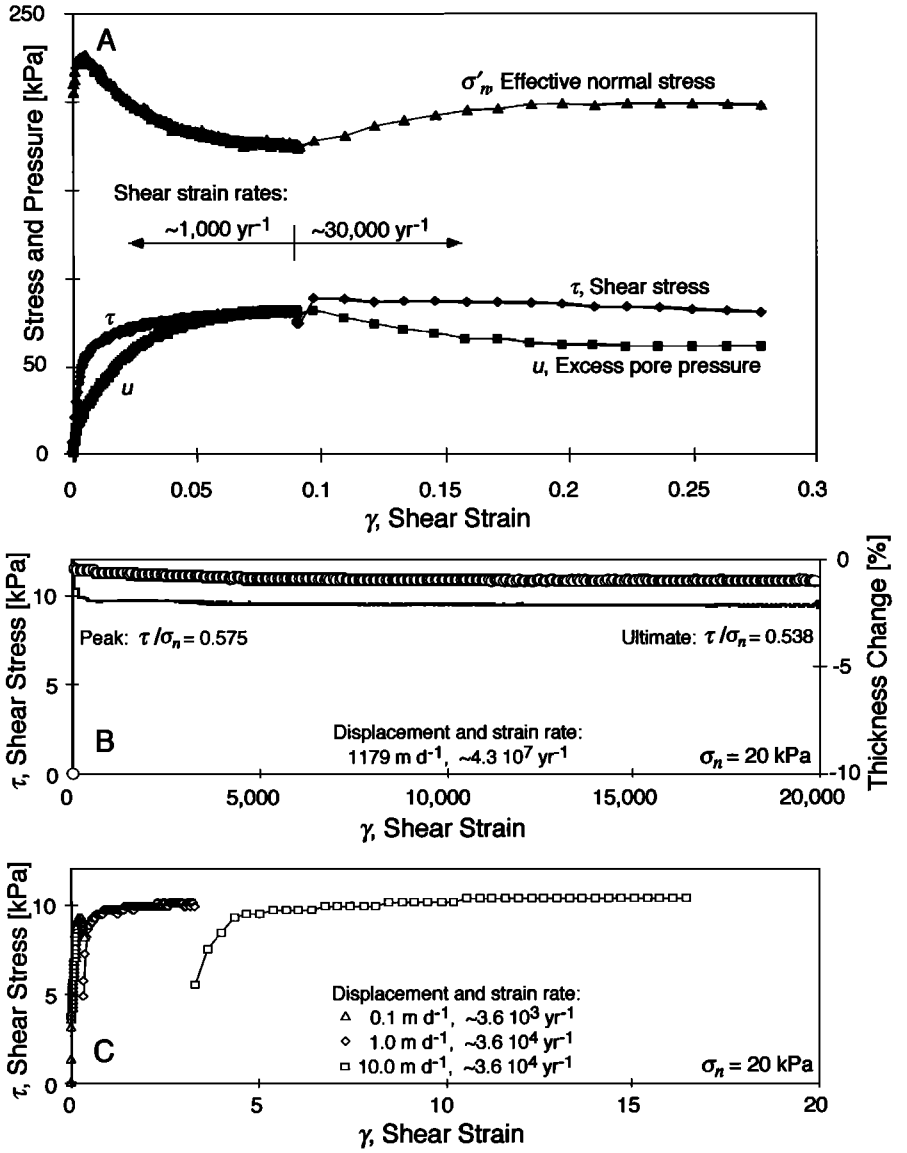

Figure 4. (a) Dependence of shear stress, excess pore pressure, and effective normal stress on shear strain in triaxial test U2. Normal effective stress, shear stress, and shear strain are calculated with (12a), (12b), (13a), and (13b) (Appendix, $\phi = 24°$). (b) Plot of shear stress (open circles, left-hand scale) and sample thickness change (solid line, right-hand scale) versus shear strain in a ring shear test. The shear strain was estimated by assuming that the relative displacement between the top and the bottom of the sample was accommodated by a homogeneous till deformation throughout the whole sample thickness of 1 cm. The negative values of sample thickness change denote sample thinning. Total normal load was set to 20 kPa. (c) Results of a ring shear test in which the relative displacement rate was increased twice by a factor of 10 from an initial low value of 0.1 m d^{-1}. Shear strain estimated as in Figure 4b.

The relatively constant value of till failure strength with strain is consistent with the prediction of critical state soil mechanics that a continuously sheared granular medium achieves a critical state in which no further changes in shear stress and volume take place [*Roscoe et al.*, 1958; *Schofield and Wroth*, 1968, p. 19]. Figure 4b demonstrates that the UpB till deformed in a ring shear device to high strains experienced little sample thickness changes beyond the initial stage of strength mobilization. The results of our ring shear tests encourage us to rely mainly on triaxial tests to reveal the mechanical behavior of the UpB till. Subsequently, we will assume that the failure state achieved in the triaxial tests at relatively low strains (~0.04) provides a sufficient approximation to the critical or residual state. This allows us to take advantage of the fact that triaxial tests, unlike shear box or ring shear tests, provide very reliable control of the effective stress state in soil samples undergoing shear.

4.2. Influence of Strain Rate and Effective Stress on Strength

We have used strain rate variations in triaxial laboratory experiments to test the proposition that the UpB till exhibits viscous behavior. Because the individual triaxial tests were performed at different levels of effective stress, data from these tests permit us

to test also the alternative, Coulomb-plastic model for the rheology of this till. Results of the tests (Figure 5) demonstrate that its strength is practically independent of strain rate and increases linearly with effective normal stress, as predicted by (1). The two Coulomb strength parameters, apparent cohesion (c_a), and internal friction (ϕ) can be calculated from principal stresses measured in a pair of triaxial tests (Appendix, equation (10)). The values of these parameters determined from three tests on undisturbed

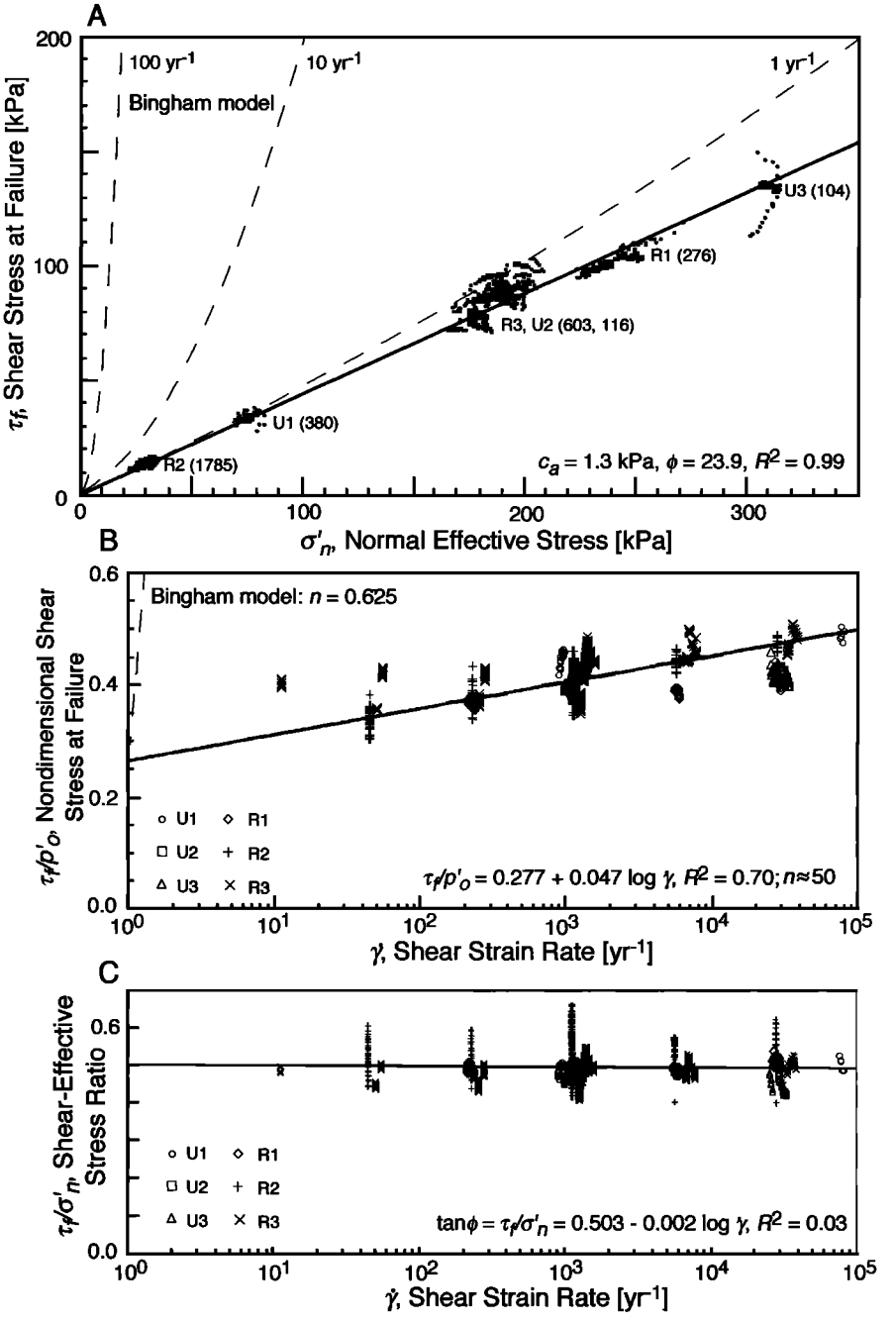

Figure 5. (a) Relationship between shear stress and normal effective stress at failure (axial strain greater than 0.04) in the six undrained triaxial tests on the UpB till in which shear strain rate was varied from ~1 yr^{-1} up to ~80,000 yr^{-1}. Numbers in parentheses give the count of data points plotted for each test. Values of shear stress and normal effective stress are calculated using (12a) and (12b) (Appendix). The solid line represents a least squares fit to the data (R^2 is the correlation coefficient). For comparison, dashed lines show the relationship between shear stress and effective stress obtained for selected strain rates from the Bingham till model of *Boulton and Hindmarsh* [1987, equation (2)]. (b) The shear stress data used in Figure 5a are normalized by the initial preconsolidation stress and plotted against the logarithm of corresponding shear strain rates (with units of yr^{-1}). The solid line gives a best fit to the data, and the dashed line illustrates again the prediction of the Bingham till model. The quantity n represents the stress exponent in a power flow law of till [*Kamb*, 1991, equation (8)]. (c) Ratio of shear stress to effective normal stress plotted against shear strain rate for the same triaxial data as in Figure 5b. This normalization removes the linear trend observed in Figure 5b and leaves the data dominated by random variations which explains the very low correlation coefficient.

samples are 3 ± 1.3 kPa and 24° ± 0.3°, respectively. The apparent cohesion is so small that we assume henceforth that it is equal to 0. The internal friction angle calculated from the same test results using the $c_a = 0$ assumption is still equal to ~24°. This magnitude of the angle is consistent with the values measured for other soils having a plasticity index similar to that of the UpB till (I_p = 15 to 16%) [*Kezdi*, 1974, Table 28; *Terzaghi et al.*, 1996, Figure 19.7].

The assumption of $c_a = 0$ makes it possible to calculate shear stress and effective normal stress on the theoretical failure planes for every data reading in the six undrained triaxial tests (Appendix, equations (12a) and (12b)). The calculated shear stress-effective stress data are fitted well by the linear Coulomb law (equation (1)) (Figure 5a). For comparison, we plot on the same figure the relationship between till strength and effective stress predicted for selected strain rates using the Bingham till model of *Boulton and Hindmarsh* [1987, Figure 7]. These predictions contrast sharply with the test results because even large changes in shear strain rate during our tests, between ca. 1 yr^{-1} to ca. 80,000 yr^{-1}, have caused no significant variation of the till shear strength (Figure 5a). The selected range of shear strain rates covers the expected range of subglacial till deformation rates [e.g., *Alley et al.*, 1986, 1987a, b]. Our data clearly show that the UpB till does not have a significant viscous behavior like the one included in the till models of *Boulton and Hindmarsh* [1987], which have been used previously to simulate the behavior of the UpB till [e.g., *Alley et al.*, 1986, 1987a, b]. Figure 5b demonstrates that the strength of the UpB till increases at most by only a few percent per each decade of increase in strain rate. This observation is consistent with previous work on soil and fault gouge rheology [*Berre and Bjerrum*, 1973, pp. 6-7; *Bishop et al.*, 1971, p. 302; *Blanpied et al.*, 1987, Figure 3; *Sheahan et al.*, 1996, Table 1; *Skempton*, 1985, p. 14]. *Kamb* [1991, equation (8)] has shown that such small strain rate dependence is equivalent to highly nonlinear, nearly plastic rheology, with a stress exponent of $n \approx 50$ to 100.

Our measurements of pore pressure demonstrate that even the observed slight changes in till strength with strain rate do not represent a true viscous effect but are caused by strain rate-induced variations in pore pressure and effective stress (Figure 4a). Increasing strain rates cause increases in effective stress and shear strength; decreasing strain rates result in the opposite trend. If till strength is interpreted in terms of the actual effective stress acting on the failure plane, the UpB till is a perfectly plastic material with failure strength determined by the frictional Coulomb relationship. The fact that pore pressure changes may account entirely for the observed changes in strength is illustrated by the ratio of shear strength to normal effective stress, which is independent of strain rate (Figure 5c). The nature of the observed pore pressure variations suggests that the till has a tendency to dilate slightly as rates of deformation increase. In undrained triaxial tests the total volume of the sample is not permitted to change and any tendency for sample expansion is counteracted by an increase in effective pressure [*Wood*, 1992, p. 26]. The corresponding strengthening of the soil sample is a byproduct of this process and is known as dilatant hardening [*Iverson et al.*, 1998].

4.3. Compressibility

We use data from confined uniaxial and triaxial tests to determine the volumetric behavior of the UpB till (Figure 6). Confined uniaxial tests simulate the type of consolidation which is the most common in nature where a soil layer is typically subjected to a vertical normal stress that changes its thickness with zero horizontal strain. This configuration is known in soil mechanics as the K_o condition [*Terzaghi et al.*, 1996, p. 104]. In contrast, till samples consolidated in preparation for standard triaxial tests experience an isotropic consolidation because the till is free to contract in all directions in response to an applied isotropic effective stress. Our results indicate that there is only a slight difference between the normal consolidation lines derived from these two types of tests (NCL_{iso} and NCL_{Ko}, Figure 6a).

The best fit lines in the e-log σ'_n space defined by measurements on overconsolidated till samples are designated as the unloading-reloading lines ($URL_{\#}$) with a number in the subscript giving the magnitude of the maximum effective normal stress to which this sample was ever subjected, σ'_{nmax} in kilopascals. We use the same line to approximate the expansion (swelling) of overconsolidated till on unloading and its compression on reloading (URL_{568}, URL_{71} in Figure 6a). This idealization neglects the fact that some irrecoverable sample compression (e decreases by ~0.001) can be observed during the several unloading-reloading cycles that we have applied to the till samples. However, the permanent compression is much smaller than the recoverable strain (e changes by ~0.01). The moduli of the NCL and URL correspond to the values of coefficients of compressibility in virgin and overconsolidated state, $C_c \cong 0.12$ and 0.15 versus $C_s \cong 0.02$, respectively. These coefficients of compressibility fall within the lower part of the range of values measured on tills and other soils [*Mitchell*, 1993, p. 170; *Sauer et al.*, 1993].

Results of our triaxial tests show that for the UpB till the CSL is located parallel and just below the NCL as observed for other soils (Figure 6a) [*Clarke*, 1987b; *Karig and Morgan*, 1992]. Sheared samples of normally consolidated till experience consolidation in drained conditions (D1) (Figure 6). In the six undrained tests, after an initial period of pore pressure relaxation, excess pore pressures built up and normal effective stresses decreased as shear strain accumulated (Figure 6b). Therefore shearing of the undrained test samples has moved their states in the e - log σ'_n space to the left of or down from their initial position on the NCL_{iso}. Because of the strain rate effects discussed previously (Figure 4a), shear-induced excess pore pressures are larger when strain rates are low and smaller when strain rates are high, for example 1000 yr^{-1} versus 30,000-80,000 yr^{-1} in Figure 5b. The CSL in Figure 6a has been obtained by best fitting e -σ'_n triaxial data collected at failure for the reference strain rate of ~1000 y^{-1}.

It is important to note that our tests have shown that the volume-change behavior of the UpB till is distinctly different from that of the Breidamerkurjokull till [*Boulton and Hindmarsh*, 1987, Figure 4]. These authors attributed a 10% increase in porosity of Breidamerkurjokull till to the influence of shear upon initially normally consolidated till. In this situation the CSL of the Breidamerkurjokull till should be placed far to the right or, equivalently, well above the NCL. This difference in volume change behavior is important because previously it has been inferred that shear-induced porosity changes in the UpB till may have the same character and magnitude as those of the Breidamerkurjokull till [*Alley et al.*, 1986, 1987a]. Moreover, the tendency of the Breidamerkurjokull till to dilate significantly during shearing has been accepted as a general property of tills that can be used as a conclusive evidence of ongoing subglacial till deformation [e.g., *Alley et al.*, 1986]. However, as in the case of the viscous behavior of the Breidamerkurjokull till, we are not able to reproduce such presumed positive dilatancy on normally

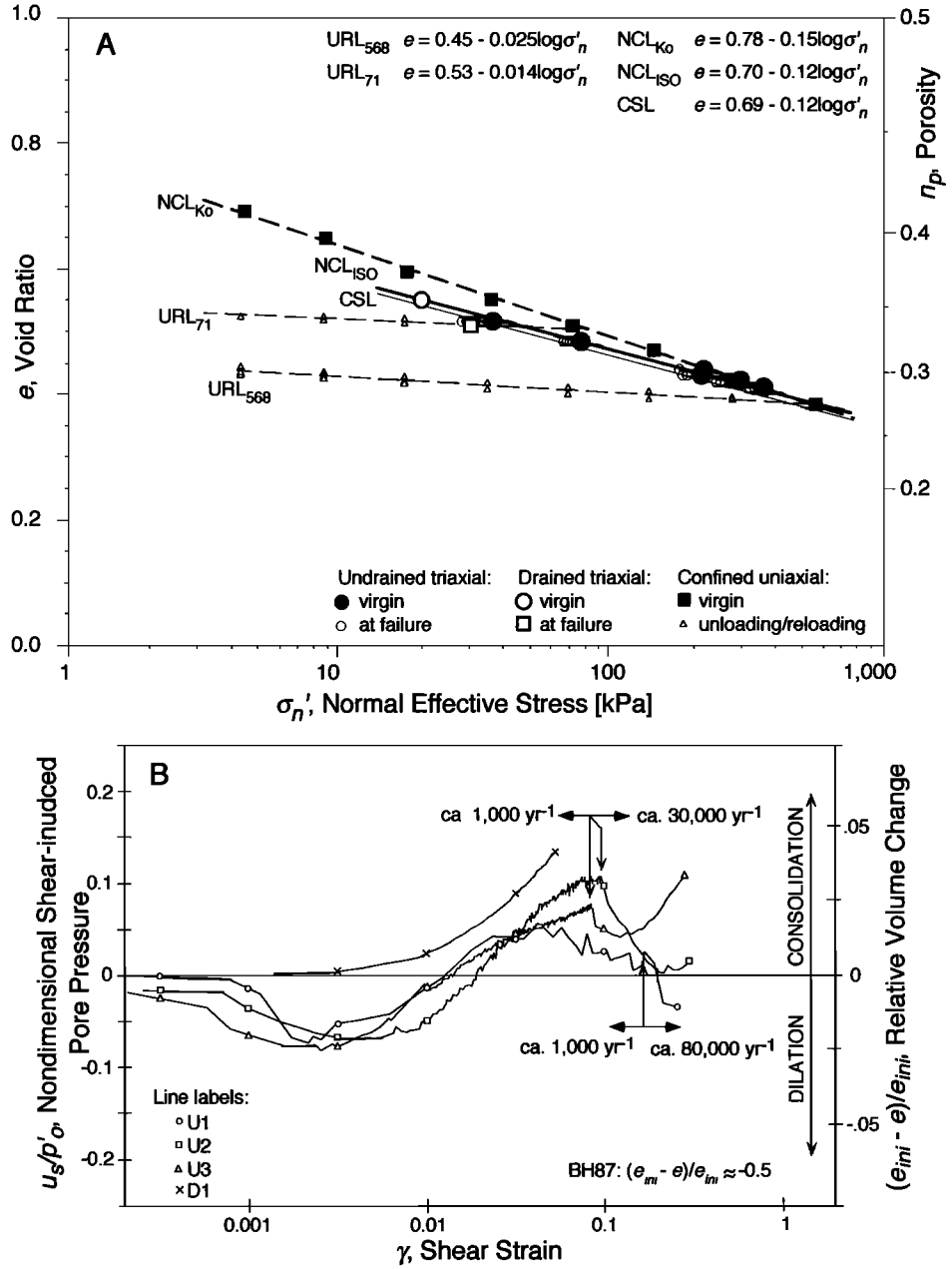

Figure 6. (a) Compressibility of the UpB till in normally consolidated (NCL), overconsolidated (URL), and sheared states (CSL). The NCL is shown for data from triaxial tests (large circles, thick solid line) and from consolidation tests (solid squares, thick dashed line). The critical state line (CSL, thin solid line) was obtained by fitting triaxial data collected at failure for the reference strain rate of 1000 yr^{-1} (small open circles drawn at every tenth observation). Behavior of the UpB till in the overconsolidated state was determined in confined uniaxial tests on two till samples preconsolidated to σ'_{nmax} = 71 kPa and σ'_{nmax} = 568 kPa, respectively (open triangles and thin dashed lines). (b) Triaxial data show shear-induced consolidation in the drained test D1, right-hand scale, which is consistent with the buildup of positive shear-induced pore pressures in undrained tests, U1, U2, and U3, left-hand scale. The three curves showing shear-induced pore pressure differ significantly from each other beyond the shear strain of ~0.15 because of increasing sample distortion that is unavoidable in triaxial tests. Shear-induced pore pressures are calculated using (14) (Appendix). For comparison, *Boulton and Hindmarsh* [1987] reported that the Breidamerkurjokull till dilates by 10% during shear, $(e_{ini} - e)/e_{ini} \approx -0.5$ in (Figure 6b).

consolidated samples of the UpB till. From the point of view of experimental evidence of soil mechanics, volume increase during shearing of normally consolidated materials is an abnormal behavior [e.g., *Karig and Morgan*, 1992]. In general, volume increases occur only during shearing of heavily overconsolidated soils [*Scott*, 1963, p. 274].

5. Compressible-Coulomb-Plastic Till Model

Laboratory test data suggest a relatively simple mechanical model of the UpB till for which both void ratio and strength are dependent on effective stress. This dependence is expressed by (1) and (2). Even the volume effective stress relation for shearing

till samples is only slightly different from that of unsheared, normally consolidated till samples. The results of our tests show that strain magnitude and strain rate have negligible influence on till strength and compressibility. Such simplification neglects some secondary effects, for example, the transient strength-mobilization stage at the initial stages of shear (strains of the order of 0.01), but is very useful in meeting our goal to investigate only the fundamental aspects of mechanical behavior of the UpB till. To the first order, just three state variables are needed to express the conditions of the UpB till at failure: (1) void ratio, (2) effective normal stress, and (3) shear strength. We call the model of till mechanics obtained by combination of equations (1) and (2), the Compressible-Coulomb-Plastic (CCP) model. The CCP model fits well into the physical framework of till mechanics proposed by *Clarke* [1987b].

Perhaps the biggest challenge of modeling the response of Coulomb-plastic till to applied stresses is posed by the fact that for plastic materials strain rates are in general not related uniquely to stresses. This represents a major departure from the viscous till model, which is based on the assumption that such a unique relationship exists. Notwithstanding this complication, we demonstrate below that when our CCP till model is subjected to realistic subglacial stress forcings, it can reproduce essential aspects of in situ till deformation.

5.1. Influence of Till Compressibility on Tiltmeter Records

In recent years detailed tiltmeter records have been collected over periods of several to a few dozens of days in tills underlying Trapridge Glacier, Yukon Territory, and Storglaciaren, Sweden [*Blake*, 1992; *Blake et al.*, 1994; *Hooke et al.*, 1997; *Iverson et al.*, 1995]. Tiltmeters are typically emplaced at depths of several decimeters below the ice base and provide a record of tilt magnitude and tilt rates. One of the most persistent features of the different tiltmeter records is the presence of tilt rate oscillations which span negative, that is, upglacier, as well as positive, that is, downglacier, values. These oscillations are temporally correlated with fluctuations in effective stress (Figures 7a and 7b) [*Hooke et al.*, 1997, Figure 2; *Iverson et al.*, 1995, Figures 1 and 2]. Negative tilt rates in subglacial tilt meter records are difficult to explain. For instance, in the viscous till model changes from positive to negative tilt rates would require basal shear stress to reverse sometimes from its typical downglacier to an upglacier direction.

The close temporal correlation between fluctuations in subglacial effective stress and tilt rate oscillations suggests that the former drive the latter (Figures 7a and 7b). Here we will show that the CCP till model provides a plausible causal link between fluctuations in normal effective stress and tilt rate oscillations. In the CCP till model, tilt rate oscillations may result solely from thickness changes experienced by a till layer when it is subjected to fluctuating normal effective stress. Our approach to simulating motion of tiltmeters in a till layer is based on the general assumption that real tiltmeters behave as passive markers that reflect faithfully any till deformation. By this assumption we exclude the possibility of till slippage occurring along the tiltmeter-till interface. Such slippage may happen in reality if the interface has a low enough friction coefficient, that is the interface would be too smooth.

From (2) it is clear that a till layer in which normal effective stress changes over some discrete time interval Δt will also experience a change in void ratio from an initial value $e_t = f(\sigma'_{n,t})$ to $e_{t+1} = f(\sigma'_{n,t+1})$. Geometric arguments can be used to show that these variations in till void ratio and till thickness result in a vertical strain (see Appendix, equation (15), for derivation):

$$\varepsilon_{n,\,t+1} = (e_t - e_{t+1})/(1 + e_t), \tag{5}$$

where strains in compression (consolidation, $e_{t+1} < e_t$) are taken to be positive and strains in extension (swelling, $e_{t+1} > e_t$) are taken to be negative. Given a nonzero vertical strain and zero horizontal strain, that is, the typical K_o condition, all planes whose initial orientation does not coincide with the three principal strain directions will experience rotation. In the case of infinitesimal rotations, the rotation angle $\Delta\Theta$ is equal to half the engineering shear strain (i.e., to the tensorial shear strain) and is given by (see Appendix, equation (16), for derivation)

$$\Delta\Theta_{t+1} = 0.5\,\gamma_{t+1} = 0.5\,\varepsilon_{n\,t+1} \sin(2\Theta_t), \tag{6}$$

where Θ_t is the initial angle of the rotating plane measured from the vertical direction. A shear strain rate, $\dot{\gamma}_{t+1}$, over a discrete time interval $\Delta t = t_{t+1} - t_t$ may be then obtained from

$$\dot{\gamma}_{t+1} = (\gamma_{t+1} - \gamma_t)/\Delta t. \tag{7}$$

Because of the nonlinearity introduced into this system of equations by the logarithmic form of (2), it is convenient to find rotations and tilt rates in response to changing effective normal stress, $\sigma'_n(t)$, by numerically integrating (2), (5), (6), and (7) through time. Since applicability of (6) is restricted to infinitesimal strains, it is necessary to select time steps small enough so that for a specific forcing function $\sigma'_n(t)$, the condition $\Delta\Theta_t < \sim 0.01$ is fulfilled at all times [*Means*, 1979, p. 151].

We first illustrate the effect of till thickness changes on tiltmeter rotations with a simple example. Figures 7c and 7d show rotations and tilt rates that would be recorded by three tiltmeters emplaced at different initial angles Θ_o into a layer of the UpB till which experiences virgin consolidation driven by a linear increase in normal effective stress (equation (2) with $C_c = 0.12$ and $e_o = 0.7$, Figure 6a). Perfectly linear changes are rare in existing records of subglacial effective stress but one can use such an idealization as a first-order approximation of the common long-term decreases or increases in this quantity (e.g., Figure 7) [*Hooke et al.*, 1997]. As shown in Figure 7, the selected linear forcing produces total rotations of several degrees and results in tilt rates that range between ~1 and 100 yr^{-1}.

Having established that till consolidation may cause large tiltmeter rotations, we hypothesize now that tiltmeters emplaced in an overconsolidated CCP till will record oscillations from negative to positive tilt rates when the till is subjected to cyclic forcing in normal effective stress. We choose to concentrate on overconsolidated till because its thickness changes are more or less recoverable (URLs in Figure 6) and should produce positive and negative tilt rate fluctuations of similar magnitude on compression and expansion, respectively. Basal water pressure records obtained parallel to the tiltmeter measurements beneath mountain glaciers show large pore pressure fluctuations [*Blake*, 1992; *Hooke et al.*, 1997; *Iverson et al.*, 1995]. This fact makes our assumption of overconsolidated state a very reasonable one because as pore pressure fluctuates up and down till is overconsolidated most of the time, because the following condition is easily met: $\sigma'_n(t) < \sigma'_{nmax}$.

To verify the plausibility of our hypothesis, we perform sample calculations for two cases that are designed to emulate (1) response of a tiltmeter emplaced 0.1 m beneath ice base in a till of low hydraulic diffusivity such as the UpB till and (2) response

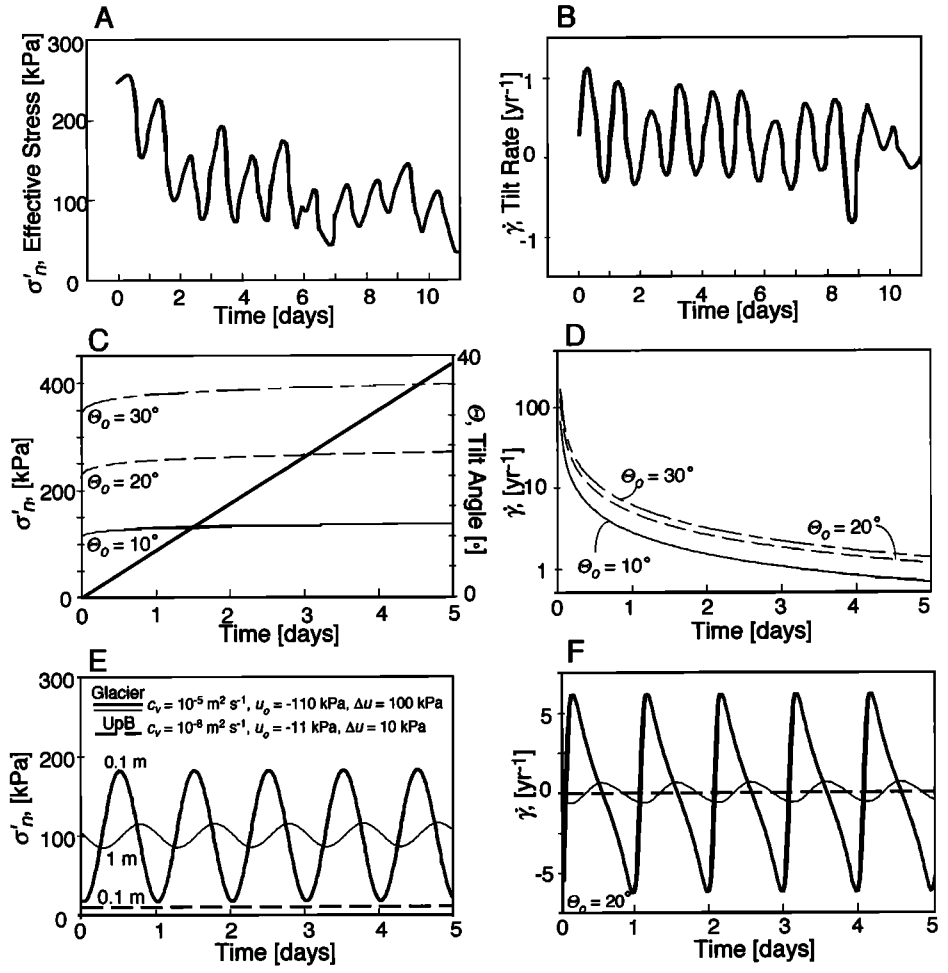

Figure 7. (a, b) Observed and (c-f) modeled changes in subglacial effective stresses and subglacial tilt rates. Figures 7a and 7b show time series of effective normal stress and tilt rate reported by *Hooke et al.* [1997, Figure 2] from the subglacial zone of Storglaciaren, Sweden. The remaining diagrams display results of our modeling in which changes in effective stresses (Figures 7c and 7e) produce tiltmeter rotations (Figures 7d and 7f), following (6) and (7). In Figure 7c, a linear increase in effective stress (thick solid line, left-hand scale) is used to drive rotation of tiltmeters which have different initial orientations (three thin lines). Figure 7d shows corresponding tilt rates for the same three tiltmeters. The second family of forcing functions considered (Figure 7e) represents diurnal fluctuations in subglacial effective stress (equations (8) and (9)). Tilt rates resulting from these stress forcings are shown in Figure 7f.

of a tiltmeter emplaced at 0.1 and 1.0 m beneath ice base in a high-diffusivity till. The second case is designed to simulate conditions beneath these mountain glaciers for which there are published tiltmeter records (e.g., Figures 7a and 7b). The hydraulic diffusivity c_v of the clay-rich UpB till is only 10^{-8} m^2 s^{-1} [*Tulaczyk*, 1998, chapter 5]. This is a low value that is probably characteristic for clay-rich tills [*Iverson et al.*, 1997]. For the hypothetical mountain glacier till we select a high value of c_v = 10^{-5} m^2 s^{-1} measured in till beneath Trapridge glacier [*Murray*, 1998]. Tills beneath other mountain glaciers are typically also coarse-grained and yield comparably high hydraulic diffusivities [*Iverson et al.*, 1997; *Murray*, 1998]. Because we could not find any reports on the compressibility coefficient C_s of tills from beneath mountain glaciers, we use in both cases the coefficient obtained in our tests on the UpB till (C_s = 0.02, Figure 6a). This is likely a conservative assumption because *Sauer et al.* [1993] have found significantly higher values of C_s for a number of tills.

In addition to the two till properties c_v and C_s we need to prescribe oscillatory effective stress forcings in both of the modeled till systems. Here we assume that the predominant component of subglacial effective stress oscillations is driven by diurnal fluctuations in basal water pressure. Such fluctuations have been observed at the bottom of Ice Stream B and beneath these mountain glaciers for which subglacial tiltmeter records were acquired [*Blake*, 1992, Figure 3.5; *Engelhardt and Kamb*, 1997; *Hooke et al.*, 1997; *Iverson et al.*, 1995]. We expect that diffusion of basal water pressure oscillations into an underlying till layer follows the classical theory of soil consolidation [*Scott*, 1963, p. 184]. After *Tulaczyk* [1999], we use in our modeling a commonly encountered solution of the one-dimensional time-dependent diffusion equation, $c_v\, u_{zz} = u_t$, with a periodic boundary condition, $u(0,t) = u_o + \Delta u \cos(\omega t)$:

$$u(z,t) = u_o + \Delta u \exp(-\psi z) \cos(\omega t - \psi z), \quad (8)$$

where $u(z,t)$ is the excess pore pressure (over hydrostatic pressure), t is the time variable, z is the vertical coordinate (Figure 2, z = 0 at the ice base), u_o is the time-averaged excess pore pressure at the top of the till (equivalent to the mean basal water pressure),

Δu is the amplitude of basal water pressure fluctuations, $\omega = 2\pi/T$, where T is the period of the fluctuations, and $\psi = [\pi/(c_v T)]^{0.5}$. The above equation for time-dependent excess pore pressure can be superposed upon a time-averaged hydrostatic effective stress increase with depth to obtain

$$\sigma'_n(z,t) = \Delta\sigma'_n z - u(z,t) \quad (9)$$

where we have assumed that the time-averaged effective stress changes linearly with depth z with $\Delta\sigma'_n = (\rho_t - \rho_w)g$ being the hydrostatic effective pressure gradient, wherein ρ_t is the till density, ρ_w is the water density, and g is the acceleration of gravity. The sign convention used in (8) and (9) assumes that pore pressures below the overburden ice pressure σ_n (Figure 2) are negative. In addition to hydrostatic conditions, one can also use (9) to consider lithostatic conditions by simply setting $\Delta\sigma'_n = 0$.

It is evident from (8) that hydraulic diffusivity c_v is a crucial parameter in modeling fluctuations of the subglacial effective stress because it determines the rate of decay of the oscillatory basal water pressure signal and its time lag with depth. This is a significant fact considering our ultimate objective to model tiltmeter behavior in the low-diffusivity till from beneath Ice Stream B and in a high-diffusivity till beneath a mountain glacier. In addition to till diffusivity, the two modeled cases have also different amplitudes of water pressure fluctuations Δu and different mean basal water pressures u_o. For the UpB till case, we choose a basal water pressure forcing with an amplitude of $\Delta u = \pm 10$ kPa around the mean average basal water pressure of $u_o = -11$ kPa. The choice of u_o is based on the preconsolidation pressures estimated by *Tulaczyk* [1998, chapter 5] for samples of the UpB till and our choice of Δu is representative of the water pressure fluctuations observed beneath Ice Stream B by *Engelhardt and Kamb* [1997, Figures 12 and 13]. In the case of the hypothetical mountain glacier till, we have used the basal water pressure data that accompany existing tiltmeter records to select representative values of $u_o = -110$ kPa and $\Delta u = \pm 100$ kPa (Figure 7a) [*Blake*, 1992, Figure 3.5; *Hooke et al.*, 1997; *Iverson et al.*, 1995].

Having equations (8) and (9) with all the necessary parameters, we are able to obtain diurnal effective stress oscillations for any depth in the two modeled tills. Figure 7e shows changes in effective stress calculated for the depth of 0.1 m in the low-diffusivity UpB till and for the depth of 0.1 and 1.0 m in the high-diffusivity till. Basal pore water pressure fluctuations are clearly unable to propagate to the relatively shallow depth of 0.1 m in the low-diffusivity UpB till but their influence is still strong at depths of 0.1 and 1.0 m in the high-diffusivity till. In the latter case, the two selected values span the range of depths at which real tiltmeters have been used to record till strain [*Blake*, 1992; *Hooke et al.*, 1997; *Iverson et al.*, 1995].

To calculate tiltmeter oscillations we use the time-dependent effective stresses shown in Figure 7e as forcing functions for the system of equations (2), (5), (6), and (7). The assumed initial tiltmeter angle with respect to the vertical direction is 20°. This value is consistent with the report of *Hooke et al.* [1997] that initial angles of tiltmeters emplaced beneath Storglaciaren were sometimes as large as 30°. Numerical time integration of the four equations yields the simulated tilt rate records given in Figure 7f. The tiltmeter emplaced at 0.1 m in the low-diffusivity UpB till remains practically motionless. However, the large effective stress fluctuations in the high-diffusivity till produce significant oscillations in tilt rate. Since we assume in our model that thickness changes of overconsolidated till are elastic, that is, reversible, no net rotation results from the cyclic effective stress forcing (Figure 7f). The most important and robust result of our calculations is the fact that by applying cyclic effective stress forcings to the CCP till we are able to reproduce tiltmeter fluctuations between negative to positive tilt rates. To this extent, the results indicate that the CCP till model provides a plausible causal link between observed fluctuations in normal effective stress and tilt rate oscillations.

Figure 7f shows tilt rate oscillations with amplitude of approximately 10 yr^{-1} and similar amplitudes are abundant in the published tiltmeter records (e.g., Figure 7b) [*Blake*, 1992; *Hooke et al.*, 1997; *Iverson et al.*, 1995]. However, the observed amplitudes of tilt rate oscillations are occasionally about an order of magnitude larger than 10 yr^{-1}. Therefore we need to estimate the maximum tilt rate amplitude that may be explained by the mechanism proposed here. Obviously, the response of simulated tiltmeters to water pressure fluctuations increases with the value of C_s. *Sauer et al.* [1993] have tested tills with C_s as high as 0.14. Fast and large water pressure changes will also produce fast tilt rates. The considered subglacial water pressure records show occasional large excursions with an amplitude of 500-700 kPa over a period of several hours [*Hooke et al.*, 1997; *Iverson et al.*, 1995]. Using these higher estimates of model parameters we have obtained tilt rate fluctuations with amplitude exceeding 100 yr^{-1}. Thus our model may account for a wide range of tilt rate oscillations, with an amplitude up to ~100 yr^{-1}.

Because we are interested here only in demonstrating the first-order aspects of our till model, we have limited ourselves to the simple cases of linear and oscillatory effective stress forcings (Figure 7). In order to reproduce subglacial tiltmeter behavior more accurately, one would have to incorporate more realistic effective stress functions (e.g., Figure 7a) and may have to include several additional processes such as (1) nonelastic thickness changes, (2) till deformation caused by the basal shear stress τ_b, and (3) inhomogeneous deformations due to till anisotropy or clast plowing. Since so little experimental and theoretical work has been done on these processes, it is practically impossible to include them at present into a more comprehensive model of till behavior. However, ongoing efforts may help allay these problems in the near future [e.g., *Iverson et al.*, 1998] (see next section of this paper).

In spite of its simplicity, our modeling demonstrates conclusively that till compressibility may have a significant effect on tiltmeters emplaced in subglacial till. Even without responding to basal shear stress, tiltmeters may experience significant rotations and oscillations caused solely by till thickness changes. These results have a significant implication for interpretations of subglacial tiltmeter records because previously it has been assumed that till is incompressible [e.g., *Blake*, 1992, p. 58] and that all tilts recorded subglacially must be caused by lateral motion of till. Finally, our calculations suggest that in the case of the UpB till layer, we should not expect the highly oscillatory tiltmeter behavior that has been observed beneath mountain glaciers. Both the low hydraulic diffusivity of this till and the nature of subglacial water pressure fluctuations should make the subglacial zone of Ice Stream B much less dynamic than the previously studied zones of mountain glaciers. This proposition may be tested in the future by instrumenting the bed of ISB with tiltmeters.

5.2. Vertical Distribution of Strain

In the previous section we have limited ourselves to modeling the response of the CCP till to changes in effective normal stress. In nature, however, there is typically a nonzero shear stress

transmitted from the ice base to the top of the till (τ_b in Figure 2). Large accumulations of total strains and large tiltmeter fluctuations recorded by instruments emplaced in deformable tills are most likely due to the combined action of fluctuating shear and normal effective stresses [*Iverson et al.*, 1998; *Tulaczyk*, 1999].

The effective stress dependence of till strength, equation (1), introduces an important complication into ice-till interactions because any vertical variations in effective stress state will cause changes in till strength distribution with depth. It is a mechanical requirement that the coupled ice-till motion should be accommodated by the weakest shear plane within a till layer. Therefore vertical variations in till strength distribution may force a vertical migration of this weakest, active shear plane. Over time, the net effect of vertical shear zone migration will be to distribute shear deformation over some thickness of the till layer. Distributed till deformation was expected to be characteristic only for tills of viscous rheology [*Alley*, 1993, p. 205]. However, shear zone migration may produce a pseudo viscous strain distribution in a Coulomb-plastic till [*Tulaczyk*, 1999, Figure 11].

Using the concept of shear zone migration, we simulate the response of the CCP till to a forcing that combines oscillatory normal effective stress with basal shear stress such that $\tau_b = \tau_{fmin} < \tau_d$ at all times. We assume that in a simulated one-dimensional column of till, ice motion is accommodated on a single horizontal shear plane that is located at the depth $z = Z_{sh}$ where the strength of the till is the least. Horizontal stress and strain gradients are assumed to be equal to zero in this till-column model. Till is treated as a homogeneous continuum. This is a reasonable assumption for matrix-dominated tills like the UpB till in which clasts make up only a few percent of total volume [*Tulaczyk et al.*, 1998]. A significant complication arises from the fact that the strength of the ice-till interface may be governed by different physics than the strength of intra till shear zones. Theoretical analysis of ice-till interactions suggests that this is a distinct possibility in the case of the fine-grained UpB till which should favor ice base sliding rather than intra till shear [*Tulaczyk*, 1999]. Because at present there are not enough observational or theoretical constraints to reliably simulate physical processes at the ice-till interface, we neglect this complication and assume that the ice-till interface has its strength determined by the same physics as any other potential shear zone within the till.

In our model, when the till is normally consolidated or lightly overconsolidated, its strength is calculated from the Coulomb equation (1) neglecting cohesion and using $\tan\phi = 0.45$ (Figure 5). We apply the Hvorslev criterion (equations (3) and (4)) only for heavily overconsolidated till with overconsolidation ratio (OVR) greater than 2 [*Wood*, 1992, pp. 198-203]. We use the Hvorslev strength parameters based on the original Hvorslev's measurements on Vienna clay, $c_{ne} = 0.1$ and $\tan\phi_e = 0.315$ [*Wood*, 1992, Table 7.1], which fall within the midrange of values for the Hvorslev parameters derived for several other soils [*Kezdi*, 1979, Table 8.2; *Wood*, 1992, Table 7.1]. Inclusion of the effect of overconsolidation on till strength is important because overconsolidation may localize strain and thus suppress shear zone migration.

Overconsolidation is the only transient effect that we include into our model of shear zone migration. There are two justifications for this decision: (1) the model focuses on large-magnitude till deformation for which the small strain transients observed in our tests are of negligible importance and (2) inclusion of strain weakening due to overconsolidation is a conservative assumption because this effect suppresses vertical shear zone migration whose plausibility we intend to demonstrate. Therefore the fact that we will be able to show vertical distribution of till deformation with a model that includes this conservative assumption strengthens our argument for the proposed concept of shear zone migration and removes one possible line of criticism. Other potential mechanisms of vertical distribution of till deformation could be introduced into this model. For example, *Iverson et al.* [1998] propose that dilatant hardening of expanding shear zones may be responsible for strain distribution in tills. In practice, including this mechanism in our model is hindered by the fact that crucial parameters of the dilatant-hardening model are yet to be constrained by field or laboratory observations. We consider here only the physical mechanisms that can be inferred from our laboratory data and treated within the CCP framework of till mechanics.

As in the previous section where we have discussed tiltmeter oscillations, subglacial effective stress functions are obtained by forcing the simulated column of till with diurnal fluctuations in basal water pressure (equations (8) and (9)). We consider the same two cases of the low-diffusivity UpB till and the hypothetical, high-diffusivity till from beneath a mountain glacier. The same values of hydraulic diffusivity, mean basal water pressure, and water pressure amplitude are used, $c_v = 10^{-8}$ m^2 s^{-1}, $u_o = -11$ kPa, and $\Delta u = \pm 10$ kPa for the UpB till case, and $c_v = 10^{-5}$ m^2 s^{-1}, $u_o = -110$ kPa, and $\Delta u = \pm 100$ kPa for the case of mountain glacier till. In contrast to our previous calculations (Figure 7), this time we compute effective stress fluctuations over a wide range of depths (Figures 8a and 9a). In this diffusional system the depth at which propagation of basal pressure oscillations ceases to be significant scales with c_v and the period of fluctuations T and is given approximately by $2(c_v T)^{0.5}$ [*Tulaczyk*, 1999]. In the low-diffusivity UpB till, the simulated diurnal basal pressure fluctuations affect only very shallow depths, ~0.06 m (Figure 8a). In the high-diffusivity case, such fluctuations can propagate down to almost 2 m depth (given by $2(c_v T)^{0.5}$). However, we have limited the modeled depth of the high-diffusivity till to 1 m because this value approximates the maximum till thickness beneath these glaciers for which till kinematics was previously studied [*Blake*, 1992; *Boulton and Hindmarsh*, 1987; *Hooke et al.*, 1997; *Iverson et al.*, 1995]. We assume that the 1-m-thick till overlies some rigid material, for example, bedrock.

The "tornado diagrams" in Figures 8a and 9a show the calculated time-dependent effective stress distribution using 1-hour timelines for the whole 24-hour cycle of basal water pressure fluctuations. We consider both lithostatic and hydrostatic conditions by setting $\Delta\sigma'_n$ in (9) equal to 0 or 10 kPa m^{-1}, respectively (under hydrostatic conditions: $\Delta\sigma'_n = (\rho_t - \rho_w)g \approx 10$ kPa m^{-1}). The two cited figures give only the results for the lithostatic conditions and show the hydrostatic effective stress gradient (dashed line) that needs to be added to each timeline of the lithostatic case to obtain the hydrostatic solution. Regardless, there is only a small difference between the two conditions because the effect of adding the small hydrostatic gradient is dwarfed by the large basal water pressure fluctuations (Figures 8a and 9a). However, we do continue to consider both the hydrostatic and lithostatic cases to demonstrate that the final conclusions of our modeling are not contingent upon the specific average effective stress gradient with depth in till.

The calculated effective stress distributions are used as input in calculations of Coulomb and Hvorslev till strength (equations (1), (3), and (4)). The results of these calculations are again shown in the same form of 1-hour timelines for the considered

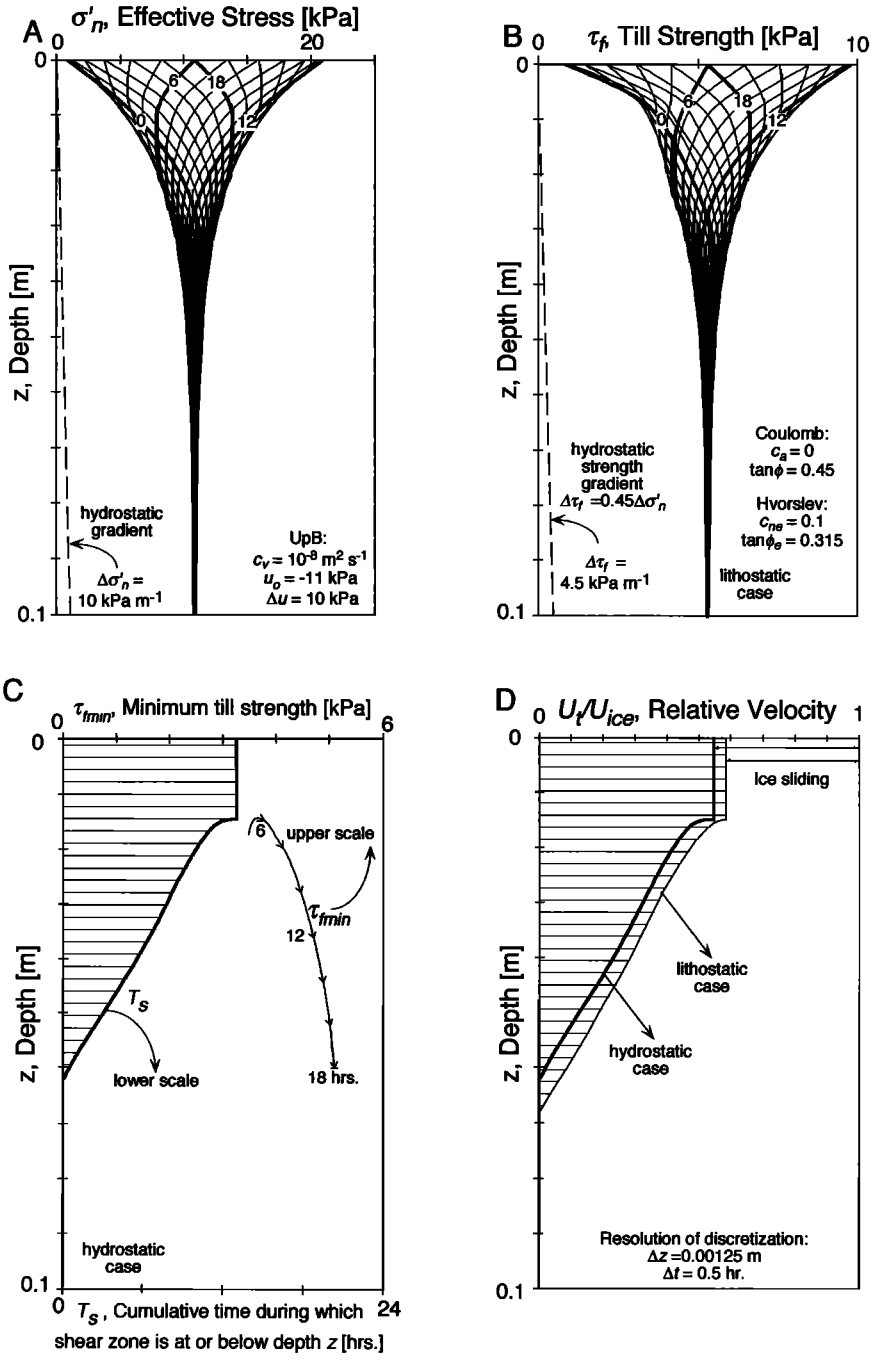

Figure 8. (a) One-hour timelines illustrating the distribution of normal effective stress with depth during a diurnal cycle of basal water pressure fluctuations (equations (8) and (9); numbers 0, 6, 12, and 18 denote hours elapsed since the beginning of the cycle). The case of lithostatic average effective stress distribution is shown and the hydrostatic case can be obtained by adding the effective stress gradient $\Delta\sigma'_n$. (b) The diurnal oscillations in effective stress (Figure 8a) trigger changes in till strength following the Coulomb criterion (equation (1)) or the Hvorslev criterion for conditions of heavy overconsolidation (equation (3)). (c) Migration of the minimum till strength with depth (thin line with arrowheads) and the cumulative time during which shear zone is at or below depth z (horizontally hatched polygon). (d) Strain distribution in till after one water pressure cycle assuming that the displacement rate across the migrating shear zone was always equal to ice velocity U_{ice}.

24-hour cycle (Figures 8b and 9b). In these two tornado diagrams the influence of overconsolidation on till strength is manifested by their slight asymmetry. This asymmetry occurs only at low effective stresses for which the threshold criterion $(\sigma'_{nmax}/\sigma'_n)$ = OVR > 2 is fulfilled and the till is treated as a Hvorslev material. This pattern of overconsolidation is, however, additionally complicated by our assumption that once motion on a given shear plane starts, any influence of previous overconsolidation is instantaneously erased and the material behaves again in a Coulomb-plastic manner. This is most apparent at the top of the

simulated till. where till strength is always determined by the simple Coulomb relationship because shear concentrates along the ice-till interface for approximately half of the water-pressure cycle (e.g., Figure 8d).

The complexity of conditions included in our modeled till system has prevented us from finding an explicit, analytical solution which would give us the position of the shear zone accommodating ice motion as a function of time. Instead, we have discretized the problem in space and time (Δt and Δz given in Figures 8d and 9d) and manually traced the shear zone migration. Following our assumption, the shear zone is always located at this depth in till where the till is the weakest. Therefore we simply determine for each time step during the 24-hour cycle the depth z for which till strength is at its minimum $\tau_f = \tau_{fmin}$. Mere inspection of the till strength timelines in Figures 8b and 9b shows that for the first 5 hours of the cycle, the minimum till strength occurs at the top of the till, $z = 0$. This condition corresponds in our model to ice sliding over the top of the till with the

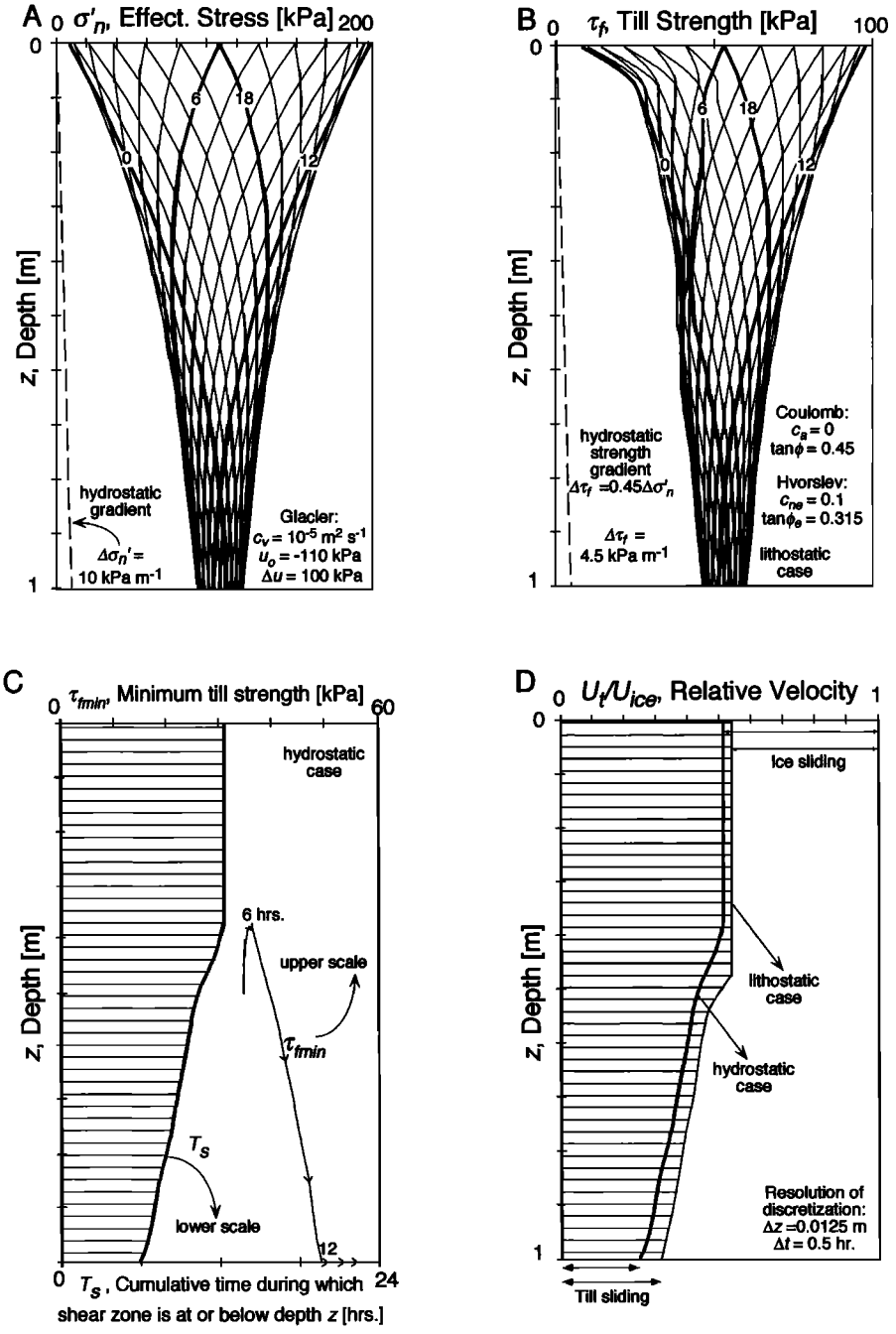

Figure 9. This figure is very similar to Figure 8. However, effective stress (Figure 9a) and till strength distribution (Figure 9b) are given here for a hypothetical high-diffusivity till experiencing relatively large basal water pressure fluctuations characteristic for basal systems of mountain glaciers. The basal water pressure fluctuations propagate through the whole assumed till thickness of 1.0 m forcing vertical migration of the minimum till strength and of the active shear zone (Figure 9c). Figure 9d shows the resulting distributed till deformation combined with ice sliding over the top of the till and with till sliding over its rigid substratum.

till layer itself remaining rigid. Subsequently, effective stress near the top of the till rises sufficiently for the minimum till strength to move down into the till column where it resides for about half of the 24-hour cycle of basal water pressure fluctuations. Migration of the minimum till strength τ_{fmin} over this part of the cycle is shown by the solid lines with arrowheads in Figures 8c and 9c. As time progresses, the depth at which the minimum till strength occurs increases. Since in the case of the high-diffusivity till we have imposed a lower till boundary at 1 m depth, the minimum till strength remains focused for a few hours along this interface. In physical terms, this condition corresponds to till sliding over the top of the assumed rigid substratum (Figure 9d). At approximately 18 hours into the water pressure cycle, the effective stress at the top of the till has again dropped down sufficiently for the minimum till strength to jump back up to $z = 0$.

Now that the path of migration for the minimum till strength (and thus for the simulated shear zone) over the considered diurnal cycle has been established, we can now construct a graph showing the cumulative time period during which the shear zone has been located at or below a given depth z (T_s in Figures 8c and 9c). At this point in our procedure it is necessary to make an assumption about the rate of motion accomodated by the shear zone in order to get the final product of our calculations, that is, graphs showing vertical distribution of till deformation after one diurnal cycle. The simplest assumption is that at all times the relative motion across the migrating shear zone is equal to a constant ice velocity U_{ice}. This assumption is justified as long as the simulated changes in the minimum till strength can be considered local, such that the total ice velocity is not influenced by the small variations in τ_{fmin} observed in our calculations. The reasonable character of this simplification may be illustrated using Ice Stream B at camp UpB as an example. There ice stream velocity appears to be determined predominantly by ice deformation in the lateral shear margins with relatively little resistance to ice motion coming from the till bed [*Echelmeyer et al.*, 1994; *Jackson and Kamb*, 1997]. It has also been shown that the observed basal water pressure fluctuations have a small influence on the velocity of Ice Stream B [*Harrison et al.*, 1993; *Engelhardt and Kamb*, 1997]. Thus if we are using the shear zone migration model to predict how strain markers may behave when they are buried in the till beneath Ice Stream B, it is justified to treat the ice stream velocity U_{ice} as an externally imposed constant parameter that is independent of the small, local variations in the shear zone strength τ_{fmin}. In the case of mountain glaciers underlain by weak till, ice deformation along the margins is probably not controlling the velocity of ice flow. However, ice deformation past bedrock knobs may play an analogous role [*Iverson et al.*, 1995].

Our assumption of constant velocity yields a simple system in which a curve giving the vertical distribution of till deformation after one diurnal cycle is equivalent to the curve showing the cumulative time period of shear zone residence below or at a given depth z (compare the hydrostatic case in Figures 8d and 9d with the plot of T_s in Figures 8c and 9c). Figures 8d and 9d give the final and most important result of our modeling because they demonstrate that a set of strain markers buried for at least one diurnal water pressure cycle in the simulated column of the CCP till would record a viscous-like profile of till velocity with depth. This viscous-like strain distribution results solely from a migration of a single shear zone whose position has been calculated by assuming plastic rheology of till with effective stress dependence of till strength. Clearly, it is not necessary to invoke viscous till rheology in order to explain existing observations of strain distribution in subglacial till layers [e.g., *Boulton and Hindmarsh*, 1987]. Even introduction of overconsolidation does not prevent the shear zone migration model from yielding vertically distributed deformation. The influence of overconsolidation is significant only in the upper part of the simulated till column where effective stress fluctuations are the largest. The migrating shear zone does not afect this part of the column that moves as a rigid plug (Figures 8d and 9d). Another complicating factor that we have considered in our simulations of vertical strain distribution in till is the presence of a hydrostatic or a lithostatic average vertical effective stress gradient. The close similarity of the results obtained for the lithostatic and hydrostatic cases shows that the fundamental outcomes of our model do not depend on the assumed effective stress gradient (Figures 8d and 9d).

The concept of shear zone migration can be tested in the future through laboratory simulations and field studies of till deformation. In the case of the subglacial zone of ISB, such a direct test with use of tiltmeters may be difficult because the dimensions of typical tiltmeters are comparable in size to the depthscale of distributed till deformation predicted by our model, ~6-7 cm. However, the results of our modeling do prompt the testable hypothesis that below this depth the UpB till is not experiencing distributed shear deformation driven by basal water pressure fluctuations. This proposition is consistent with the result of a recent borehole experiment performed in the UpB area. The experiment indicated that most of ice stream velocity is accommodated within no more than several centimeters from the ice base [*Engelhardt and Kamb*, 1998]. Our estimate of the deforming till thickness is 2 orders of magnitude smaller than the previous estimate made with an assumption of viscous rheology for the UpB till [*Alley et al.*, 1986, 1987a, b]. Field tests of the shear zone migration model will be more feasible in deforming till layers observed beneath several mountain glaciers. These till layers reach thicknesses of up to 0.6 m permitting measurements of vertical distribution of strain and effective stress with readily available instruments. We expect that such measurements will reveal a picture of subglacial till behavior that is more complex than that provided by the simplified, first-order models presented here. For instance, clast plowing and dilatant hardening may provide additional mechanisms that contribute to the vertical distribution of strain [*Iverson et al.*, 1998; *Tulaczyk*, 1999]. Nevertheless, future subglacial observations may verify whether the CCP till model can be used to explain the relation between stress variability and distributed till deformation.

6. Conclusions

New triaxial and ring-shear tests performed on samples of the UpB till corroborate the nearly plastic till rheology determined earlier in shear box tests on this material [*Kamb*, 1991]. These test results dispel important doubts about the generality of this finding by demonstrating that the mechanical behavior of this till is neither strongly dependent on strain magnitude nor on sample or test geometry. Moreover, undrained triaxial tests with pore pressure measurements reveal that even the small observed strain rate dependence of till strength is caused by variations in pore pressure rather than by true viscous effects. If the failure strength of the till is interpreted in terms of the actual normal effective stress on failure planes, then the UpB till can be characterized as a perfectly plastic Coulomb material. The till strength increases approximately linearly with normal effective stress ($\tau_f \approx 0.45\sigma'_n$) but is relatively insensitive not only to strain rate but also to strain magnitude. The difference between peak and ultimate till strength measured in two ring shear tests was only 6% and 8%.

This low sensitivity of strength to strain magnitude demonstrates that results of small and medium strain tests, for example, triaxial or shear box tests (maximum strains of ~0.1 and ~1), can be used as reliable approximations of high-strain behavior of the UpB till. Comparisons of our test results with published results of analogous tests show consistently that the mechanical behavior of the UpB till is very similar to the behavior of soils in general. This fact encourages use of concepts from soil mechanics in building qualitative understanding and quantitative models of subglacial till behavior.

Based on the results of our laboratory tests, we formulate a Compressible-Coulomb-Plastic (CCP) till model, consisting of two relationships: the linear dependence of till strength on normal effective stress, and the logarithmic dependence of void ratio on normal effective stress. By applying realistic, time-dependent stress forcings to a simulated column of the CCP till, we are able to reproduce two fundamental aspects of the existing subglacial tiltmeter and strain marker records: (1) oscillations of tilt rates between negative and positive values and (2) net rotation of tiltmeters and viscous-like vertical distribution of aggregate deformation in till. In the framework of the CCP model the oscillatory behavior of tiltmeters represents a byproduct of vertical thinning and thickening of overconsolidated till in response to a cyclic effective stress forcing. Net tiltmeter rotations of up to several degrees are produced in our till model during virgin consolidation. In addition, viscous-like vertical distribution of strain may be produced in a column of the CCP till when the till is subjected to an oscillatory effective stress forcing combined with shear stress that is equal to the till strength. The depth to which these two mechanisms distribute deformation in a till layer is controlled by the hydraulic diffusivity of the till c_v and by the period of basal water pressure fluctuations T (the characteristic depth scale is given by $2(c_v T)^{0.5}$). Because of the very low hydraulic diffusivity of the UpB till ($c_v \approx 10^{-8}$ m^2 s^{-1}), we predict that till deformation driven by the basal water pressure fluctuations observed beneath Ice Stream B is restricted to depths of only several centimeters beneath the ice base. This depth is an order of magnitude less than the thickness of subglacial shear zones observed in high-diffusivity tills beneath mountain glaciers, 0.1-0.6 m [*Boulton and Hindmarsh*, 1987; *Hooke et al.*, 1997; *Iverson et al.*, 1995]. It is also 2 orders of magnitude less than the thickness of the actively deforming till layer deduced for this ice stream from a combination of seismic data and the viscous till model, ~6 m [*Alley et al.*, 1986, 1987a, b].

In spite of the fact that in the past soil mechanics tests were frequently discounted as a potential tool for studying till mechanics, our results indicate that there are no fundamental inconsistencies between the existing body of observations constraining in situ till behavior and the experimentally constrained Coulomb-plastic till rheology. Thus we hypothesize that subglacial till deformation and ice-till interactions may be simulated using models of till mechanics based on laboratory test results, such as the CCP model. Our hypothesis may be verified by future laboratory and field investigations of other tills. Pending such verification, we propose the CCP model of the UpB till as the framework for understanding and modeling motion of the West Antarctic ice streams.

Appendix: Derivations of Equations

In this appendix we explain derivations of several important equations that are not widely used in glaciological literature. The first part of this appendix relates to our evaluation of the effective normal stress, shear stress, shear strain, and shear-induced pore pressure from the principal stresses and strains measured in the triaxial tests (equations (10) through (13)). In the second part we devise a method for calculating tilt rates from changes in till thickness (equations (15) and (16)).

One can show from the Mohr circle construction that apparent cohesion c_a and internal friction angle ϕ are related to the major and minor principal effective stresses at failure σ'_{1f} and σ'_{3f} [*Scott*, 1963, equation (8-10b)]:

$$(\sigma'_{1f} - \sigma'_{3f})/2 = c_a \cos\phi + [(\sigma'_{1f} + \sigma'_{3f})/2] \sin\phi. \quad (10)$$

Since this equation has two unknowns, at least two triaxial test results are needed to calculate c_a and ϕ. For materials with negligible apparent cohesion, (11) simplifies to a form that has only one unknown ϕ and requires only a single pair of σ'_{1f}, and σ'_{3f} to solve for it. To calculate the effective normal stress on any plane with its normal at Θ degrees to the direction of the major effective stress, we can use [*Means*, 1979, equation (9.4)]

$$\sigma'_n = 0.5(\sigma'_{1f} + \sigma'_{3f}) + 0.5(\sigma'_{1f} - \sigma'_{3f}) \cos(2\Theta). \quad (11)$$

Failure planes in a Coulomb material with an angle of internal friction ϕ have orientation $\Theta = 45° + 0.5\phi$ and $-45° - 05\phi$, sign convention as by *Means* [1979, Figure 9.5]. Making use of (10), the expression for normal effective stress acting on failure planes in a cohesionless soil may be expressed purely in terms of principal stresses:

$$\sigma'_n = \sigma'_{3f}(1 + \sin\phi) = 2\,\sigma'_{1f}\sigma'_{3f}/(\sigma'_{1f} + \sigma'_{3f}). \quad (12a)$$

Moreover, (1), (10), and (12a) can be combined to show that the shear stress on failure planes is related to principal stresses through

$$\tau_f = (\sigma'_{1f}\sigma'_{3f})^{0.5}(\sigma'_{1f} - \sigma'_{3f})(\sigma'_{1f} + \sigma'_{3f})^{-1}. \quad (12b)$$

The Mohr circle construction for infinitesimal strains shows that engineering shear strain accumulated on failure planes over some time interval Δt can be calculated from the major and minor principal strains ε_1 and ε_3 [*Means*, 1979, Figure 16-3]:

$$\gamma = (\varepsilon_1 - \varepsilon_3)\sin(2\Theta) = (\varepsilon_1 - \varepsilon_3)\sin(0.5\pi + \phi)$$

$$= (\varepsilon_1 - \varepsilon_3)\cos\phi. \quad (13a)$$

In the configuration of a triaxial test one can assume that the axial strain $\Delta L/L_i = \varepsilon_1$, is the major principal strain and the radial strain, $\Delta R/R_i = \varepsilon_3$ is the minor principal strain. The symbols ΔL, ΔR, L_i, and R_i represent the changes in sample length and radius and the initial sample length and radius before the time Δt elapsed, respectively. Data from a standard triaxial test evaluate directly only the axial strain ε_1 [*Bishop and Henkel*, 1957, p. 28]. The minor, radial strain can be related to the axial strain through the conservation of volume, $V_{i+1} = V_i + \Delta V$:

$$\varepsilon_3 = 1 - \{[(1 - \varepsilon_1)^{-1}][1 + \Delta V(\pi R_i^2 L_i)^{-1}]\}^{0.5}, \quad (13b)$$

where ΔV is measured in drained triaxial tests and it is equal to zero in undrained tests. Substitution of (13b) into (13a) yields the expression that permits calculation of engineering shear strain on failure planes from triaxial test data, for example, Figure 4a.

When pore pressure is measured in triaxial tests, its changes can be attributed to a combination of changes in both the mean stress and the deviatoric stress. In studies of soil dilatancy, it is important to isolate the pore pressure changes induced by shear because these changes reveal whether the tested soil samples show tendency to expand or contract upon shearing. The shear-induced pore pressures u_s are calculated from triaxial data with the following equation [*Sheahan et al.*, 1996, p. 102]:

$$u_s = p_w - (\sigma_1 + 2\sigma_3)/3, \quad (14)$$

where p_w is the total pore water pressure measured during the test, and σ_1, σ_3 denote the major and minor principal total stresses, respectively.

In order to derive an equation which gives vertical strain in a till layer with time variable void ratio, that is, equation (5), we assume the K_o consolidation and swelling of a till layer. The requirement of no horizontal strain yields the following identity:

$$\varepsilon_{n,\,t+1} = \Delta Z/Z_t = (V_t - V_{t+1})/V_t, \qquad (15)$$

where $\varepsilon_{n,t+1}$ is the vertical strain at time t_{t+1}, ΔZ is the till thickness change over the time step Δt, Z_t is the till thickness at $t_t = t_{t+1} - \Delta t$, and V_t, V_{t+1} are till volumes at the corresponding times, t_t and t_{t+1}. The expression for $\Delta Z = V_t - V_{t+1}$ was selected to obtain positive vertical strains when till experiences consolidation, that is its thickness and volume decrease from t_t to t_{t+1}. It can now be observed that for a saturated till with negligible compressibility of water and solid particles, the total volumes, $V_t = V_s + V_{w,t}$ and $V_{t+1} = V_s + V_{w,t}$, are a summation of a nonvariable volume of till solids, $V_{s,t} = V_{s,t+1} = V_s$, with the variable volumes of pore water, $V_{w,t}$ and $V_{w,t+1}$. Using the definition of void ratio, $e = V_w/V_s$, we can substitute $V_t = (1 + e_t)V_s$ and $V_{t+1} = (1 + e_{t+1})V_s$ into (15) to obtain the desired equation (5). Furthermore, from Mohr circle one can note that when the minor principal strain is equal to zero, the following expression gives the infinitesmal engineering shear strain for a line inclined at Θ degrees to the major principal direction, that is, the vertical direction in our problem [*Means*, 1979, equation (16.3)]:

$$\gamma = \varepsilon_t \sin(2\Theta). \qquad (16)$$

Geometrically, the engineering shear strain is the change in angle between two initially perpendicular lines, for example at Θ and $90° + \Theta$. For calculations of tilt magnitudes and tilt rates, equations (6) and (7), we want to have an expression for $\Delta\Theta$, that is, the change in angle between the vertical direction and the line inclined initially at Θ.

Acknowledgments. This project was funded by grant OPP-9219279 from the National Science Foundation to B. Kamb and H. Engelhardt. Ronald F Scott of the Division of Engineering and Applied Science at the California Institute of Technology has generously contributed equipment and expertise at many stages of this project His help was especially vital during the design and construction of the ring shear device We are thankful to Less Fruth and the management of Earth Technology, Inc., Irvine, California, for making available their triaxial testing laboratory. This paper benefited from helpful comments provided by Neil Humphrey, Neal Iverson, and Joseph Walder.

References

Alley, R.B., How can low-pressure channels and deforming tills coexist subglacially, *J. Glaciol.*, *38*, 200-207, 1993.

Alley, R B , D.D Blankenship, C R Bentley, and S.T. Rooney, Deformation of till beneath Ice Stream B, West Antarctica, *Nature*, *322*, 57-59, 1986.

Alley, R.B , D.D Blankenship, S T. Rooney, and C.R. Bentley, Till beneath Ice Stream B, 3, Till deformation: Evidence and implications, *J. Geophys. Res.*, *92*, 8921-8929, 1987a.

Alley, R.B., D D. Blankenship, S.T. Rooney, and C R. Bentley, Till beneath Ice Stream B, 4, A coupled ice-till flow model, *J Geophys. Res.*, *92*, 8931-8940, 1987b.

Anayi, J.T., J.R. Boyce, and C.D.F. Rogers, Modified Bromhead ring shear apparatus, *Geotech. Test. J*, *12*, 171-173, 1989.

Bentley, C.R., Antarctic ice streams: A review, *J. Geophys. Res.*, *92*, 8843-8858, 1987.

Bentley, C.R., Rapid sea-level rise soon from West Antarctic Ice Sheet collapse, *Science*, *275*, 1077-1078, 1997.

Berre, T., and L. Bjerrum, Shear strength of normally consolidated clays, *Proc. 8th Int. Conf. Soil Mech. Found. Eng.*, *1*, 39-49, 1973.

Bindschadler, R., West Antarctic Ice Sheet collapse, *Science*, *276*, 242-246, 1997.

Bindschadler, R., Monitoring ice sheet behavior from space, *Rev Geophys.*, *36*, 79-104, 1998.

Bishop, W., and D.J. Henkel, *The Measurement of Soil Properties in the Triaxial Test*, Edward Arnold, London, 1957.

Bishop, W., G.E. Green, V.K. Garga, A. Andresen, and J.D. Brown, A new ring shear apparatus and its application to the measurement of residual strength, *Geotechnique*, *12*, 273-328, 1971.

Blake, E.W., The deforming bed beneath a surge-type glacier: measurement of mechanical and electrical properties, Ph.D. thesis, Univ. of B. C., Vancouver, Canada, 1992.

Blake, E.W., U.H. Fischer, and G.K C. Clarke, Direct measurement of sliding at the glacier bed, *J. Glaciol.*, *40*, 595-599, 1994.

Blankenship, D.D., C.R. Bentley, S.T Rooney, and R.B. Alley, Seismic measurements reveal a saturated porous layer beneath an active Antarctic ice stream, *Nature*, *322*, 54-57, 1986.

Blankenship, D.D., C.R. Bentley, S.T. Rooney, and R.B., Alley, Till beneath Ice Stream B, I, Properties derived from seismic travel times, *J. Geophys. Res.*, *92*, 8903-8911, 1987.

Blanpied, M.L., T.E. Tullis, and J.D Weeks, Frictional behavior of granite at low and high sliding velocity, *Geophys. Res. Lett.*, *14*, 554-557, 1987

Boulton, G.S., and R.C.A. Hindmarsh, Sediment deformation beneath glaciers; Rheology and geophysical consequences, *J. Geophys. Res.*, *92*, 9059-9082, 1987.

Bowles, J E., *Engineering Properties of Soils and Their Measurement*, McGraw-Hill, New York, 1992.

Bromhead, E.N., A simple ring shear apparatus, *Ground Eng.*, *12*, 40-44, 1979.

Clark, P.U , Surface form of the southern Laurentide Ice Sheet and its implications to ice sheet dynamics, *Geol. Soc. Am. Bull.*, *104*, 595-605, 1992.

Clarke, G.K.C., Fast glacier flow: Ice streams, surging, and tidewater glaciers, *J. Geophys. Res.*, *92*, 8835-8841, 1987a.

Clarke, G.K.C., Subglacial till: A physical framework for its properties and processes, *J. Geophys. Res.*, *92*, 9023-9037, 1987b.

Cuffey, K., and R.B. Alley, Is erosion by deforming subglacial sediments significant? (toward till continuity), *Ann. Glaciol.*, *22*, 17-24, 1996.

Echelmeyer, K A., W.D. Harrison, C. Larsen, and J.E. Mitchell, The role of the margins in the dynamics of an active ice stream, *J. Glaciol.*, *40*, 527-538, 1994.

Engelhardt, H., and B. Kamb, Basal hydraulic system of a West Antarctic ice stream: Constrains from borehole observations, *J Glaciol.*, *43*, 207-230, 1997.

Engelhardt, H., and B. Kamb, Sliding velocity of Ice Stream B, *J. Glaciol.*, *44*, 223-230, 1998.

Engelhardt, H., N. Humphrey, B. Kamb, and M. Fahnestock, Physical conditions at the base of a fast moving Antarctic ice stream, *Science*, *248*, 57-59, 1990.

Harrison, W.D., K.A. Echelmeyer, and H. Engelhardt, Short-period observations of speed, strain and seismicity on Ice Stream B, Antarctica, *J. Glaciol.*, 39, 463-470, 1993.

Hooke, R.L., B. Hanson, N.R. Iverson, P. Jansson, and U.H Fischer, Rheology of till beneath Storglaciaren, Sweden, *J. Glaciol.*, *43*, 172-179, 1997.

Hughes, T., Can ice sheets trigger abrupt climatic change?, *Arct. Alp. Res.*, *28*, 448-465, 1996.

Iverson, N.R., B. Hanson, R.L. Hooke, and P. Jansson, Flow mechanism of glaciers on soft beds, *Science*, *267*, 80-81, 1995.

Iverson, N.R., R.W. Baker, and T.S. Hooyer, A ring-shear device for the study of till deformation. Tests on till with contrasting clay contents, *Quat. Sci. Rev.*, *16*, 1057-1066, 1997.

Iverson, N.R., T S Hooyer, and R.W. Baker, Ring-shear studies of till deformation: Coulomb plastic behavior and distributed strain in glacier beds, *J Glaciol.*, *44*, 634-642, 1998.

Jackson, M., and B. Kamb, The marginal shear stress of Ice Stream B, West Antarctica, *J. Glaciol.*, *43*, 415-426, 1997.

Jones, M., Mechanical principles of sediment deformation, in *The Geologic Deformation of Sediments*, edited by A. Maltman, pp. 37-72, Chapman and Hall, New York, 1992.

Kamb, B., Rheological nonlinearity and flow instability in the deforming-bed mechanism of ice stream motion, *J. Geophys. Res.*, *96*, 16,585-16,595, 1991.

Karig, D., and J. Morgan, Tectonic deformation: Stress paths and strain histories, in *The Geologic Deformation of Sediments*, edited by A. Maltman, pp. 167-204, Chapman and Hall, New York, 1992.

Kezdi, A., *Handbook of Soil Mechanics*, Elsevier Sci., New York, 1974.

MacAyeal, D.R., Irregular oscillations of the West Antarctic Ice Sheet, *Nature*, *359*, 29-32, 1992.

Means, W.D., *Stress and Strain. Basic Concepts of Continuum Mechanics for Geologists*, Springer-Verlag, New York, 1979.

Mitchell, J.K., *Fundamentals of Soil Behavior*, John Wiley, New York, 1993

Murray, T., Assessing the paradigm shift: Deformable glacier beds, *Quat. Sci. Rev.*, *16*, 995-1016, 1998.

Paterson, W.S.B., *The Physics of Glaciers*, 3rd ed., Pergamon, Tarrytown, N.Y., 1994.

Roscoe, K.H., A.N. Schofield, and C.P. Wroth, On the yielding of soils, *Geotechnique*, *8*, 22-52, 1958

Sauer, E.K., A.K. Egeland, and E.A. Christiansen, Preconsolidation of tills and intertill clays by glacial loading in southern Saskatchewan, Canada, *Can. J. Earth Sci.*, *30*, 420-430, 1993.

Schofield, A.N, and C.P. Wroth, *Critical State Soil Mechanics*, McGraw-Hill, New York, 1968

Scott, R F., *Principles of Soil Mechanics*, Addison-Wesley-Longman, Reading, Mass., 1963.

Sheahan, T.C., C.C. Ladd, and J. T. Germaine, Rate-dependent undrained shear behavior of saturated clay, *J. Geotech Eng.*, *122*, 99-108, 1996.

Skempton, A W, Residual strength of clays in landslides, folded strata and laboratory, *Geotechnique*, *35*, 3-18, 1985

Stark, T.D., and J.J. Vettel, Bromhead ring shear test procedure, *Geotech. Test. J.*, *15*, 24-32, 1992

Terzaghi, K, R.B. Peck, and G. Mesri, *Soil Mechanics in Engineering Practice*, John Wiley, New York, 1996.

Tulaczyk, S., Basal mechanics and geologic record of ice streaming, West Antarctica, Ph.D. thesis, 371 pp., Calif. Inst. of Technol., Pasadena, 1998.

Tulaczyk, S., Ice sliding over weak, fine-grained tills. Dependence of ice-till interactions on till granulometry, in *Glacial Processes, Past and Modern*, edited by D.M. Mickelson and J. Attig, *Spec. Pap. Geol. Soc. Am.*, *337*, 159-177, 1999.

Tulaczyk, S., B. Kamb, R.P. Scherer, and H F. Engelhardt, Sedimentary processes beneath a West Antarctic ice stream; constraints from textural and compositional properties of subglacial debris, *J. Sediment Res.*, *68*, 487-496, 1998.

Tulaczyk, S., W.B. Kamb, and H.F. Engelhardt, Basal mechanics of Ice Stream B, West Antarctica, 2, Undrained plastic bed model, *J Geophys. Res.*, this issue.

Whillans, I.M., and C.J. van der Veen, New and improved determinations of velocity of Ice Stream B and Ice Stream C, *J. Glaciol.*, *39*, 483-490, 1993.

Whittle, A.J., and M J. Kavvadas, Formulation of MIT-E3 constitutive model for overconsolidated clays· *J. Geotech Eng.*, *120*, 174-198, 1994.

Wood, D M., *Soil Behaviour and Critical State Soil Mechanics*, Cambridge Univ. Press, New York, 1992

H.F. Engelhardt and W.B. Kamb, Division of Geological and Planetary Sciences, California Institute of Technology, Pasadena, CA 91125. (hermann@gps.caltech.edu, barclay@gps.caltech.edu.)

S. Tulaczyk, Department of Geological Sciences, University of Kentucky, 101 Slone Bldg., Lexington, KY 40506 (smtula0@pop uky.edu.)

(Received August 6, 1998; revised March 3, 1999; accepted July 20, 1999.)